分类号： 密级：公开

UDC 学号：2021024558

華南師範大學

South China Normal University

硕士学位论文

（学术学位）

Study of the Twist- 3 Gluon Contribution to Sivers Asymmetry in J/ψ Production in SIDIS

学 位 申 请 人：陈隆杰

专 业 名 称：粒子物理与原子核物理

研 究 方 向：核子结构

所 在 院 系：量子物质研究院

导师姓名及职称：Shinsuke Yoshida 副研究员

2024 年 5 月 4 日

华南师范大学研究生学位论文答辩合格证明

学位申请人 陈隆杰 向本学位论文答辩委员会提交题为 Study of the Twist-3 Gluon Contribution to Sivers Asymmetry in J/ψ Production in SIDIS 的硕士论文，经答辩委员会审议，本论文答辩合格，特此证明。

硕士学位论文答辩委员会成员名单

姓名	职称	单位	备注
陈龙斌	副教授	广州大学	主席
邢宏喜	研究员	华南师范大学	委员
梁剑	研究员	华南师范大学	委员

论文指导老师： Shinsuke Yoshida

华南师范大学 量子物质研究院（公章）

2024 年 5 月 9 日

（此页须放在提交版论文封面后第一页，纸质版装订，电子版放入彩色扫描件）

Study of the Twist-3 Gluon Contribution to Sivers Asymmetry in J/ψ Production in SIDIS

专业名称： 粒子物理与原子核物理

申请者： 陈隆杰

导师： Shinsuke Yoshida

摘 要

自微扰量子色动力学 (p-QCD) 被确立为研究核子内强相互作用力的基本方法以来，有关核子内部结构的研究一直是基础物理学的研究重点。近半个世纪以来，通过 p-QCD 框架对实验数据的分析研究，目前已积累了大量成果。尽管如此，核子内部结构仍存有大量反常现象，特别是作为核子组分的胶子的作用。自 2000 年来相关实验主要在相对论离子对撞 (RHIC) 实验上进行，运行至今已取得了包括质子自旋测量在内的大量成果。而有关自旋的两个难题则一直未能在 RHIC 实验中被彻底解决，其中之一为自旋难题，另一为单横向自旋不对称 (SSA) 。质子自旋难题首次于 1987 年被欧洲缪子合作组 (EMC) 实验所发现，所观测到的夸克自旋对质子自旋贡献很小 (4% ~ 24%)。尽管有人初步地认为主要贡献应该来自质子的三个价夸克，但实验数据与这种粗略的假定相悖。此外，前文所提到的 RHIC 实验也证实了胶子自旋亦不占主要贡献，故深入了解其他可能的源头是解决这一难题的关键。一般的，SSA 被定义为散射过程中只有一个横向极化的强子参与的自旋极化现象。传统的 p-QCD 计算预测 SSA 应小于 0.1% 进而在高能散射中可忽略不计。而实验数据则证伪了这一观点，且在七十年代后期所观测到的极化超子产物中，SSA 最高可达 10%。由于 p-QCD 已被广泛应用于高能散射中且成功解释了众多实验现象，故理论预测与实验的偏差表明有关核子结构仍需投入大量研究工

作。而过去几十年内 RHIC 所提供的关于 SSA 实验数据极大地推动了 p-QCD 框架的发展。其中由部分子 (夸克胶子) 的自旋和轨道运动所产生的 Sivers 效应可能是较高 SSA 的起源。一般的它可被拆分为夸克 Sivers 效应及胶子 Sivers 效应，得益于 HERMES 实验与 COMPASS 实验中 ep 散射所积累的数据，前者已通过被广泛地研究讨论过了。由于实验数据的缺乏，有关胶子 Sivers 效应的研究则并未得到充分关注，故仍然有较大的研究空间。此外，由于胶子 Sivers 效应描述了胶子轨道运动，了解其机理将促进对不对称度的研究。未来有关质子自旋的研究将由中美两国建造下一代实验设施，电子离子对撞机 (EIC) 实验所继承。它将为知之甚少的胶子 Sivers 效应研究提供实验数据，与之相关的理论研究将会愈发重要。

目前存在两类描述胶子 Sivers 效应的框架，其中一类引入了末态强子中部分子的横动量相关的依赖性 (transverse momentum dependence)，而另一类则引入了扭度为 3 的共线极限展开 (twist-3 expansion at collinear limit)。前者提供了研究末态夸克胶子低横动量 (低 p_T) 区间内三维空间运动的手段，后者则为研究硬散射中相干部分子间的关联提供工具。这两种框架依末态 p_T 的不同而有不同的适用范围。在本论文中，我们将计算在 semi-inclusive DIS (SIDIS) 情形时 J/ψ 产物中 twist-3 展开中胶子对 SSA 的贡献，将在 EIC 条件下对两个不同的模型进行相应数值模拟，以阐明 J/ψ 产物中 twist-3 展开中胶子对单自旋不对称度的贡献。我们的结果表明，末态夸克对的强子化效应在 SSA 的层面上消失了。此外，J/ψ SSA 是研究与胶子横向动量分布相关的 C-even 类型 twist-3 胶子分布函数的理想观测对象。直接计算表明，在散射截面公式中 C-odd 类型贡献相互抵消了，同时 SSA 在较高横动量区间内并未消失。SSA 可展开为五个归一化的结构函数，基于现有模型在对 SSA 进行数值模拟时，我们发现其中一个归一化函数 $\frac{\mathcal{F}_1}{2\sigma_1^{\mathrm{U}}}$ 具有显著的贡献，最高可达 10%，可能是较大 SSA 的源头。本文为未来 EIC 实验上研究 SSA 提供了理论预测，并提供了一种新的研究思路。

关键词： p-QCD, Twist-3 展开, 单自旋不对称度, Sivers 效应

Study of the Twist-3 Gluon Contribution to Sivers Asymmetry in J/ψ Production in SIDIS

Major： Particle Physics and Nuclear Physics

Name： Longjie Chen

Supervisor： Shinsuke Yoshida

ABSTRACT

Studies of the nucleon's internal structure have been one of major research trends in the fundamental physics since the perturbative quantum chromodynamics (p-QCD) was confirmed to be the fundamental theory in describing the strong interaction. Numerous findings on the nucleon structure have been accumulated through investigations of experimental data within the perturbative approach to the strong interaction (p-QCD) in the past half century. Notwithstanding, there still exists many mysteries, specifically, in the gluon's role as a constituent of the nucleon. Modern investigations of the nucleon structure have been conducted by Relativistic Heavy Ion Collider (RHIC) which started in 2000. Many achievements, including the measurement of the gluon's spin, have been made since it started. However, two longstanding spin problems, the proton spin puzzle and the single transverse-spin asymmetry (SSA), have not been completely solved at RHIC. The construction of the proton spin was realised as a problem in 1987 by the European Muon Collaboration (EMC) experiment where the measured quark spin contribution was found to be small ($4\% \sim 24\%$) to the proton spin. Although one may naïvely think that the main contribution arises from the three valence quarks of the proton, experimental

observation contradicted this naïve expectation. The aforementioned RHIC experiment clarified that the gluon spin is also not enough to the proton spin. Further investigation of other possible sources is needed to solve the puzzle. The SSA is the spin phenomenon defined in a scattering process in which only one of hadrons is transversely polarized. A p-QCD calculation once demonstrated that the SSA should be less than 0.1% and, therefore, negligible in high energy scatterings. However, tens of percent asymmetries were experimentally observed in pion production and transversely polarized hyperon production in the late 70s. This fact was accepted as a mystery in high energy QCD because the traditional p-QCD calculation had been very successful in many other high energy scatterings. RHIC experiment has provided much new data on the SSA, which well motivated the development of the perturbative QCD framework in the past couple of decades. The Sivers effect generated by the correlation between spin and orbital motion of partons inside the proton has been recently studied as a possible origin of large SSA. The Sivers effect can be categorized into quark type and gluon type.The quark Sivers effect has been well studied so far in proton-proton collision at RHIC and electron-proton collision at HERMES and COMPASS. On the other hand, the gluon type still leaves much room for research because of the absence of relevant experimental data. Further investigations of the above spin problems will be inherited by the next generation collider experiments, Electron-Ion Colliders (EICs) in the U. S. and China. Therefore theoretical studies related to these experiments will continue to grow in importance.

There are two types of the p-QCD frameworks to describe the Sivers effect on the SSA. The transverse momentum dependent (TMD) factorization introduces the transverse momentum of partons inside a hadron. Another successful framework is the twist-3 contributions in the collinear expansion which describes coherent correlations among partons in a hard scattering. Those frameworks have different applicable regions with respect to the transverse momentum of an observed hadron. In this thesis we will carry out calculations for the gluon Sivers type contribution to the SSA within the twist-3 framework in J/ψ productions at semi-inclusive deep inelastic scattering (SIDIS). We will also perform

numerical simulations for the SSA at the EIC energy in order to clarify the role of twist-3 gluon contribution in the J/ψ production. Our result shows that the effect of hadronizing of final quark pair vanishes in the level of SSA. Besides, the J/ψ SSA is an ideal observable to investigate the C-even type twist-3 gluon distribution that has a direct relationship with the gluon transverse-momentum-dependent distribution function. We also discover that C-odd type contribution is directly cancelled in the spin-dependent cross section formula while the SSA doesn't vanish in high p_T regions. SSA can be expanded into five normalized structure functions, and based on the existing model, we find that one of the normalized functions, $\frac{\mathcal{F}_1}{2\sigma_1^{\mathrm{U}}}$, has a significant contribution,up to which could be the source of a large SSA. In this thesis we provide a theoretical prediction for the future experimental study of SSA in EIC, and provides a new research idea.

KEY WORDS: p-QCD, Twist-3 Expansion, Single Spin Asymmetry, Sivers effect

Contents

Figure List

Symbol List

q	momentum transfer
$\sigma^{\text{unpol/pol}}$	unpolarized/polarized cross section formula
p_T	transverse momentum of the j/ψ
$f_i(x), i = u, d, s. \cdots$	parton distribution function
A_N	single spin asymmetry
N_c	number of color degrees of freedom

Chapter 1 Introduction

1.1 Background

Discovery of the proton can be tracked back to 1917 when E. Rutherford performed the scattering of nitrogen atom and α particle[1]. Another crucial discovery was made 15 years later by J. Chadwick in his prominent paper[2] with an announcement on possible existence of the new particle named neutron. Those nucleons were first accepted as elementary particles in nature. However, a large number of new nucleon-like particles(hadrons in the present day)[3] were discovered with the development of experimental technologies, which revealed that the nucleons are not the most fundamental building blocks and motivated searches for more elementary constituents inside the nucleons. Tremendous effort was devoted to the clarification of the constituents without the known fundamental theory for the strong interaction. Some important concepts were advocated around 60s. The quark model was first proposed by Gell-Mann and Zweig in 1964 [4, 5] to give a unified picture in describing a number of hadrons. A straightforward way to investigate the proton's internal structure is deep-inelastic scattering(DIS) in which an electron penetrates deep into the proton and then the cross section reflects the information about the proton's internal structure. DIS process, $ep \rightarrow eX$, is illustrated in FIG 1.1 where X represents the unobserved particles and $q = (\ell - \ell')$ denotes the momentum of the virtual photon emitted from the electron. W describes the scattering between the proton and the virtual photon. In 1968 Bjorken pointed out the scaling behaviour in the ratio of the cross sections for the proton scattering and for the scattering of a point-like charged particle(Mott scattering) in large q^2 regime shown in FIG1.2[6]. The scaling rule has suggested that the proton is composed of point-like particles in high energy scatterings. From this observation, Feynman illustrated the parton picture[7] in which the scattering of a proton can be expressed by incoherent scatterings of free partons shown as FIG1.3. Although the concept of free partons had not been accepted first because it is far from the

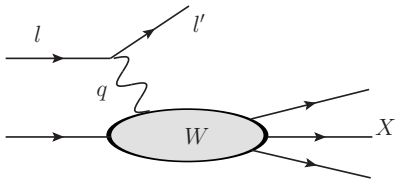

FIG 1.1 A schematic diagram for DIS process.

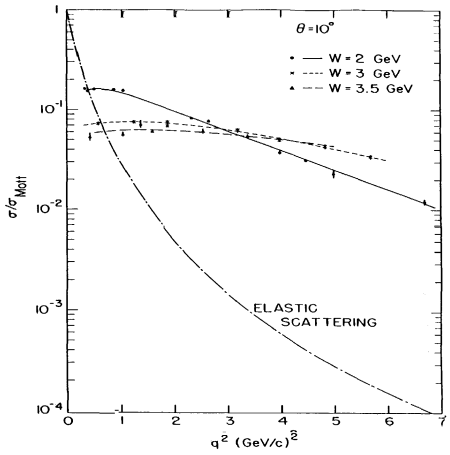

FIG 1.2 Scaling behaviour of charged particles in proton scatterings, discovered by Bjorken and Paschos.

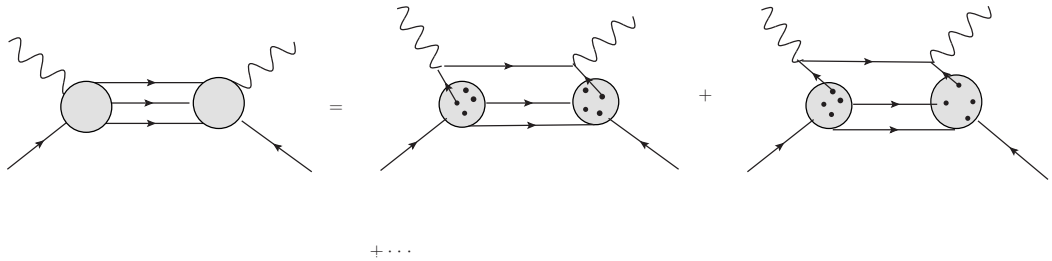

FIG 1.3 The scattering of particles in parton model induced by Feynman.

image of the strong interaction, it was finally supported by the birth of quantumchromodynamics(QCD) as the fundamental theory of the strong force and the discovery of the asymptotic freedom in 1973[8]. In DIS, one can decompose the whole scattering into the lepton part and the hadron part, thus we can deal with them independently. The contribution at leading-order(LO) with respect to the strong coupling constant is illustrated in FIG1.4 The hadronic part can be written in terms of two independent structure functions

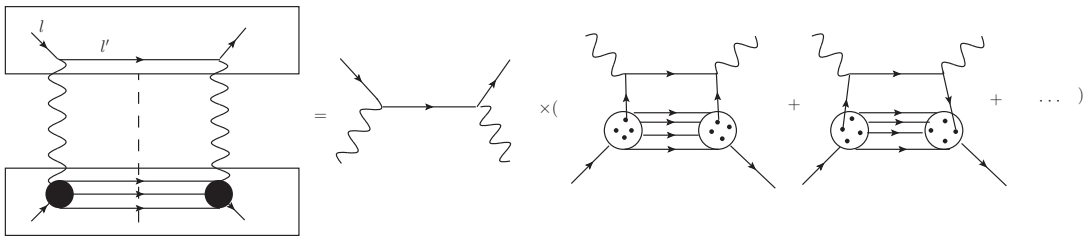

FIG 1.4 Full picture of the high energy scattering in parton model.

from the Lorentz covariance,

$$W^{\mu\nu} = F_1(p\cdot q, q^2)\left(\frac{q^\mu q^\nu}{q^2} - g^{\mu\nu}\right) + F_2(p\cdot q, q^2)\frac{1}{p\cdot q}\left(p^\mu - \frac{p\cdot q}{q^2}q^\mu\right)\left(p^\nu - \frac{p\cdot q}{q^2}q^\nu\right). \quad (1.1)$$

One can check that the hadronic tensor stated before shall satisfy Ward identity securing the gauge invariance. The parton model predicts that the structure functions should obey the following Callan-Gross relation[9] in the large q^2 limit.

$$F_1(p\cdot q, q^2) = \frac{F_2(p\cdot q, q^2)}{2x_B} = \sum_{i=q,\bar{q}} e_i^2 f_i(x_B), \quad (1.2)$$

where $f_i(x_B)$ is the parton distribution function(PDF) with flavor i and the Bjorken variable x_B is given by $-q^2/(2p\cdot q)$. Relevant experimental data[10] confirmed the relation as shown in FIG 1.5. Further understanding of the nucleon structure was provided by

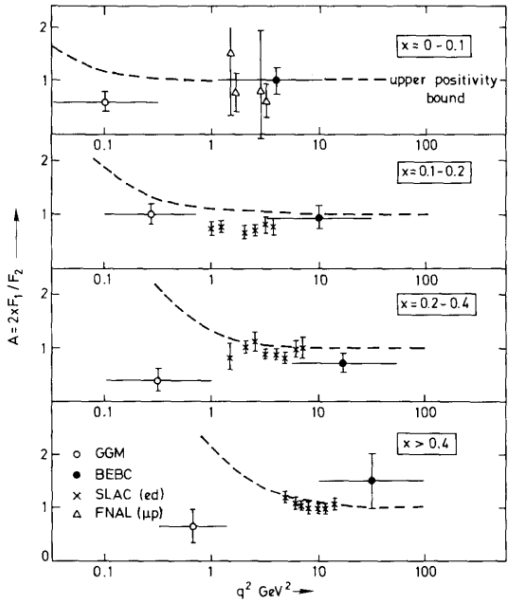

FIG 1.5 Experimental data that has confirmed the Callan-Gross relation, conducted by Bosetti *et al.*.

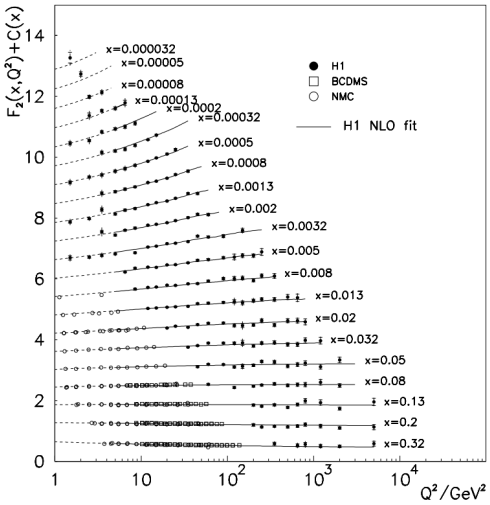

FIG 1.6 Behaviour of the scaling violation, observed by Aid *et al.*.

subsequent experiments. The experimental data from HERA[11] shown as FIG 1.6 has indicated that the scaling behaviour of the structure function is violated particularly in the small x_B region. This scaling violation of the structure function reflects the fact that the PDFs have the energy scale dependence. This scale dependence can be naturally given

as the renormalization group equation obtained through the factorization of the infra-red divergence appears in the next-to-leading(NLO) order contribution. This renormalization group equation[12], also known as DGLAP evolution equation, successfully reproduced the observed scaling violation, which is one of the important successes in the early stage of the QCD phenomenology. The parton model combined with higher order QCD corrections has been established as the basic perturbative technique for high energy hadron scatterings. Many hadronic reactions, not only DIS but also purely hadronic reactions in RHIC and LHC, have been successfully explained to date.

Despite of many successes, the basic perturbative calculation could not describe the single transverse-spin asymmetry(SSA) at all. The single transverse-spin asymmetry is defined in a process in which only one hadron is transversely polarized. Here we explain the SSA in pion production in the proton-proton collision as one of the examples,

$$p + p^{\uparrow} \to \pi + X, \tag{1.3}$$

where $p^{\uparrow}$ denotes the transversely polarized proton. The SSA (A_N) is defined as the asymmetry of the cross section for the transverse spin given as follows where $\uparrow$ & $\downarrow$ denote different directions of polarization.

$$A_N = \frac{d\sigma^{\uparrow} - d\sigma^{\downarrow}}{d\sigma^{\uparrow} + d\sigma^{\downarrow}}. \tag{1.4}$$

In parton model, each scattered parton has the same polarization state with the parent hadron. Thus the LO contribution arises from the following quark scattering.

$$q + q^{\uparrow} \to q + q. \tag{1.5}$$

The initial transverse spin has to vanish in the final state, which is caused by the small quark mass m_q(a few MeV for u, d quarks) effect. Since A_N is a dimensionless quantity, it is roughly given by[13],

$$A_N \sim \frac{m_q}{p_T}. \tag{1.6}$$

In the RHIC experiment[14], the transverse momentum p_T is the order of GeV. Then the asymmery A_N is negligible, which was the prediction from the traditional parton model calculation. However, the observed asymmetries in the RHIC shown in FIG 1.7[15]

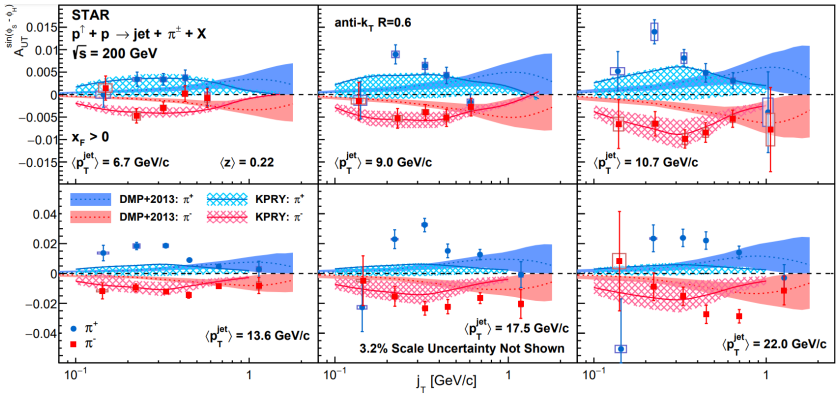

FIG 1.7 Asymmetries observed in $pp^{\uparrow}$ collisions in the exploring of spin structure, brought by Lin Ting.

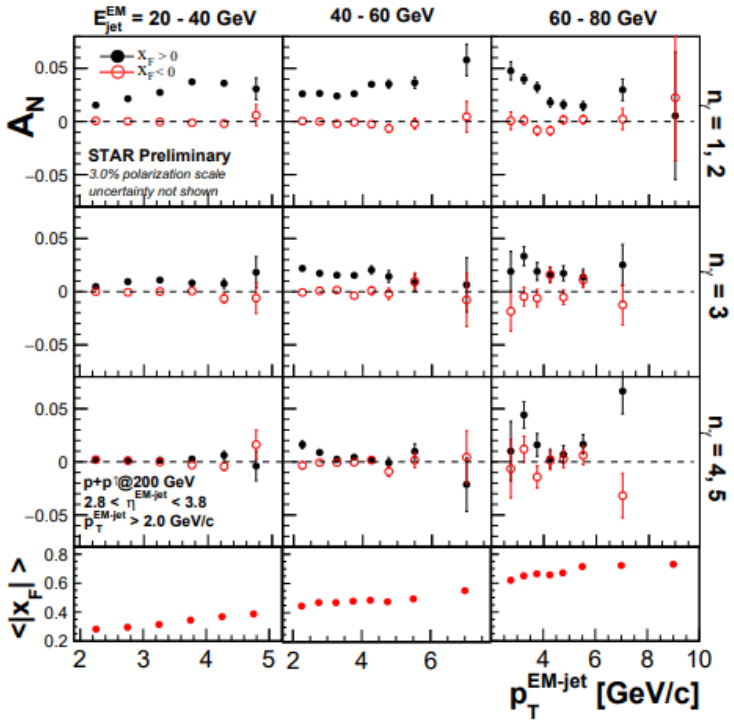

FIG 1.8 Experimental data about the single spin asymmetry in $pp^{\uparrow}$ collisions, observed by Liang Xilin.

and FIG 1.8[16] completely contradict the prediction. The origin of the SSA has been a longstanding problem since it was first observed in late 70s. Solving this problem is one

of the main goals of the next collider experiments, Electron-Ion collider experiments in the U. S. and China. The development of the perturbative QCD framework is needed for those next generation experiments.

1.2 Research Status

Almost half a century has passed since the first observation of the large SSA. It is now convinced that transverse momenta of partons and correlations among them, which are not considered in the traditional p-QCD calculation, play a role in the emergence of the large SSA. Quark distribution functions are defined by the proton's matrix element of two quark or two gluon fields. If we introduce the transverse momentum of an internal parton k_T, we can see the appearance of a new function as follows:

$$\mathcal{F}.\mathcal{T}.\langle pS_\perp|\bar{\psi}(0)\gamma^\mu\psi(x^-,x_T)|pS_\perp\rangle = \frac{2}{M_N}\epsilon^{\mu\nu\rho\sigma}p_\nu k_{T\rho}S_{\perp\sigma}f_{1T}^\perp(x,k_T)\cdots, \tag{1.7}$$

where $\mathcal{F}.\mathcal{T}.$ stands for Fourier transformation, $|pS_\perp\rangle$ is the state vector of the transversely polarized proton, ψ, $\bar{\psi}$ are quark fields and $f_{1T}^\perp(x,k_T)$ is the distribution function called Sivers function[17]. The effect of the Sivers function is generated in the case that an unpolarized parton inside the transversely polarized proton participates in the parton scattering. We find that this nontrivial polarization difference between an internal parton and the parent proton provides a novel way to solve the aforementioned problem, none of quarks in the parton scattering is transversely polarized and therefore, the small quark mass m_q is not needed to generate the SSA. The Sivers effect could appear with the nonperturbative QCD scale $\Lambda_{\rm QCD}$. Thus the expected asymmetry is hundreds time larger than that in the conventional calculation and could be source of the large SSA.

$$A_N \sim \frac{m_q}{p_T} \quad \rightarrow \quad \frac{\Lambda_{\rm QCD}}{P_\pi^\perp}, \tag{1.8}$$

which could reproduce the observed large asymmetries in the experiments[18]. The perturbative QCD framework taking k_T into account is called transverse-momentum-dependent(TMD) factorization framework. The TMD framework offers a first principle QCD

calculation when the transverse momentum of an observed hadron in the final state $P_h^\perp$ is small compared to the hard scale of the process. Experimental data in the small $P_h^\perp$ region were provided by electron-proton collision at HERMES and COMPASS[19–21]. The quark Sivers distribution function has been well understood in the past couple of decades attributed to the accumulated experimental data.

There is another way to implement a similar effect in the SSA. We consider a proton matrix element of more than two operators as[22, 23]

$$\mathcal{F}.\mathcal{T}.\langle pS_\perp|\bar{\psi}(0)\gamma^\mu gF^{\alpha+}(y^-)\psi(x^-)|pS_\perp\rangle = -\frac{M_N}{2}\epsilon^{\alpha\beta-+}p^\mu S_{\perp\beta}F_{FT}(x_1,x_2)+\cdots, \quad (1.9)$$

where g is the strong coupling constant, $F^{\alpha+}$ is a field strength of gluon and $F_{FT}(x_1, x_2)$ is called the colinear twist-3 function. This twist-3 function also gives a similar contribution to the TMD Sivers function, the scattering of an unpolarized parton inside the transversely polarized proton. The twist-3 contribution generates an incoherent scattering of partons, a couple of partons inside the proton participate in the same scattering which is not considered in the parton model. The twist-3 framework in the collinear factorization also offers a first principle calculation when, in contrast to TMD framework, $P_h^\perp$ is large so that it can be regarded as the hard scale. RHIC experiment has reported much data on the SSA in the high $P_h^\perp$ region. These two frameworks aforementioned reflect different mechanisms for the productions of final observables in terms of $P_h^\perp$. The quark twist-3 distribution function has been well understood through the analysis of the RHIC data[24, 25] to date.

Successes of the above new p-QCD frameworks have suggested that the SSA leads to deeper understandings of the nucleon structure which were overlooked in the traditional parton picture like the transverse momenta of partons and the incoherent correlations among them. We can define the gluon type Sivers effect by replacing all quark fields in the above matrix elements with the field strength tensors of gluon. Although the quark Sivers effect has been well understood in the past couple of decades, little about the gluon Sivers has been understood because of the absence of relevant experimental data. The understanding of the gluon Sivers effect is a challenging task of future ex-

periments. The U. S. and China are planning next generation experiments, Electron-Ion colliders(EICs)[26, 27]. Much new data for the SSA in the electron-proton collision is expected to be reported in the near future. A distinct feature of the EIC compared to the previous electron-proton collision experiments is its ability to cover the high $P_h^\perp$ region where the twist -3 framework is valid and unique. An ideal observable to investigate the gluon structure inside the proton is the cross section in a heavy meson production because the heavy quark hadronizing into the heavy meson is mainly produced by a gluon inside proton. In the case of the gluon Sivers effect, the SSA in a heavy meson production is an ideal observable. In this thesis, we'll discuss the SSA in the J/ψ production in the electron-proton collision. A lot of papers have been published based on the TMD framework because the existing experiments cover the small $P_h^\perp$ region, while no work has been done within the twist-3 framework. We show our first derivation of an analytical formula for the J/ψ SSA and perform some numerical simulations on them at the typical EIC energy. Our work will contribute to the understanding of the gluon Sivers effect through the future analysis of the data from the EICs.

The remainder of this thesis is organized as follows: Chapter 1 is devoted to a brief introduction. Chapter 2 illustrates relevant definitions of kinematical variables in SIDIS and calculation of the twist-3 contribution in the collinear expansion. Chapter 3 shows the derivation of the formula for the SSA in J/ψ production in detail. Chapter 4 shows our numerical simulations on the J/ψ SSA and end up with the summary of this thesis.

Chapter 2 Twist Calculation

In this chapter we demonstrate the collinear expansion[28] up to the twist-3 level in DIS as one of examples.

2.1 Collinear expansion

In parton model one can recall that the cross section in DIS can be decomposed into the leptonic part and hadronic part. Only the hadronic part is relevant in the collinear expansion and the leptonic part is universal. We first start with a set of diagrams shown in the following figure, where the upper blobs represents hard scatterings between the virtual

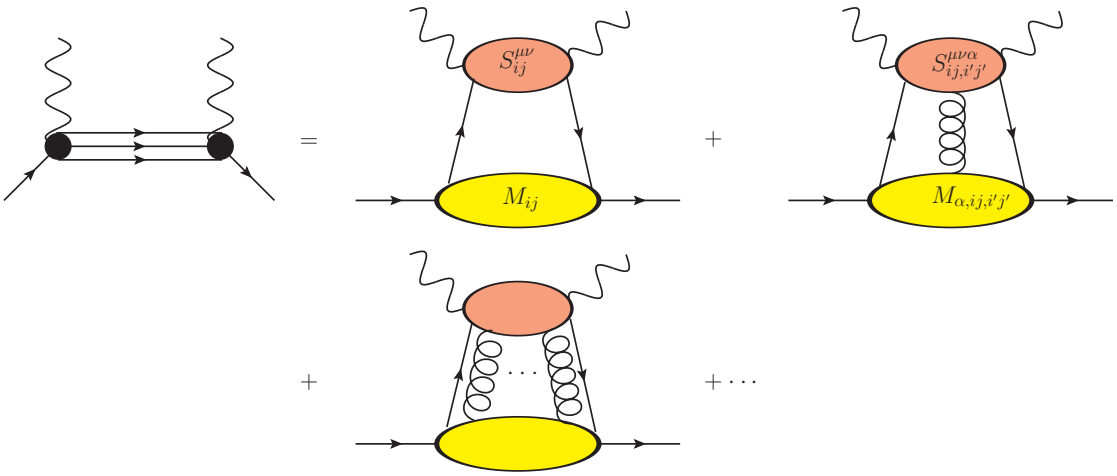

FIG 2.1 Generic diagrams for the hadronic part.

photon and partons, lower blobs illustrates the non-perturbative proton matrix elements of quark and gluon fields, i', j' denote indices of the color SU(3) group, μ, ν are the Lorentz indices of the external virtual photon lines and i, j... are indices in the spinor space. The explicit forms of the proton matrix elements are respectively given by

$$\begin{aligned} &\text{diagram 1}: \quad \int \frac{d^4k}{(2\pi)^4} S_{1,ji}(k) M_{1ij}(k), \\ &\text{diagram 2}: \quad \int \frac{d^4k_1}{(2\pi)^4} \int \frac{d^4k_2}{(2\pi)^4} S^{a,\alpha}_{2,ji,j'i'}(k_1,k_2) M^{a}_{2,\alpha,ij,i'j'}(k_1,k_2). \end{aligned} \tag{2.1}$$

where a denotes the adjoint color index, $k_1(k_2)$ represents the momentum of the incoming (outgoing) quark participating in the hard scattering. The virtual photon indices μ, ν are omitted for simplicity. One can easily give mathematical expressions to more gluon-linked diagrams appear in the expansion. Only the above diagrams are relevant in our derivation. The proton matrix element in each diagram is mathematically expressed by

$$\begin{aligned} M_{1,ij}(k) &= \int d^4\xi e^{ik\cdot\xi}\langle p|\bar{\psi}_j(0)\psi_i(\xi)|p\rangle, \\ M^a_{2,\alpha,ij,i'j'}(k_1,k_2) &= \int d^4\xi_1 e^{ik_1\cdot\xi_1}\int d^4\xi_2 e^{i(k_2-k_1)\cdot\xi_2}\langle p|\bar{\psi}_{jj'}(0)gA^a_\alpha(\xi_2)\psi_{ii'}(\xi_1)|p\rangle \end{aligned} \tag{2.2}$$

$S_{1,2}$ represent hard scatterings of the photon and partons. Here we show the explicit forms of the hard parts $S_{1,ji}, S^{a,\alpha}_{2,ij,i'j'}$ in DIS in massless case. Based on the Feynman rules for

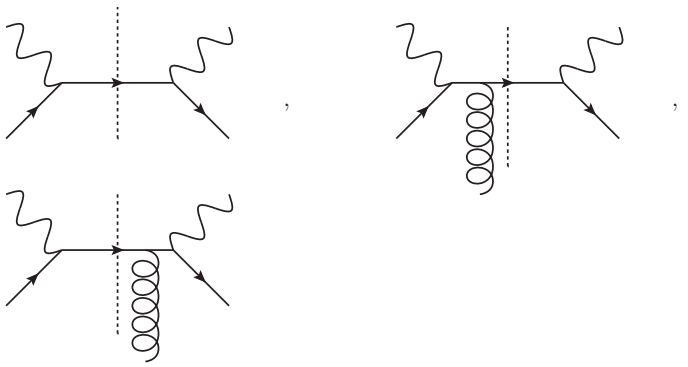

FIG 2.2 Hard scattering part.

QCD[29], we can show

$$\begin{aligned} S_{1,ji}(k) &= \left(\gamma^\rho\,(\not{k}+\not{q})\,\gamma^\sigma\right)_{ji}2\pi\delta\Big((k+q)^2\Big), \\ S^{a,\alpha}_{2ji,j'i'}(k_1,k_2) &= -\Big(\gamma^\rho\,(\not{k}_2+\not{q})\,\gamma^\alpha\frac{1}{\not{k}_1+\not{q}}\gamma^\sigma\Big)_{ji}2\pi\delta\Big((k_2+q)^2\Big)(\mathrm{T}^a)_{j'i'} \\ &\quad -\Big(\gamma^\rho\frac{1}{\not{k}_2+\not{q}}\gamma^\alpha(\not{k}_1+\not{q})\gamma^\sigma\Big)_{ji}2\pi\delta\Big((k_1+q)^2\Big)(\mathrm{T}^a)_{j'i'}. \end{aligned} \tag{2.3}$$

where T^a denotes the Gell-Mann matrices and $\delta(\cdots)$ is the on-shell condition of the final state quark. Through the identity,

$$(\not{k}_2 - \not{k}_1) = (\not{k}_2 + \not{q}) - (\not{k}_1 + \not{q}). \tag{2.4}$$

we can derive the Ward-Takahashi identity as

$$(k_2 - k_1)_\alpha S^{a,\alpha}_{2ji,j'i'}(k_1, k_2) = (S_{1,ji}(k_2) - S_{1,ji}(k_1))(\mathrm{T}^a)_{j'i'}. \tag{2.5}$$

This identity identifies the relations between $S_{1,ji}(k_i)\&S^{a,\alpha}_{2ji,j'i'}(k_1, k_2)$ that will play a crucial role throughout the calculation. One can find that momenta $k_{1,2}$ are integral variables and don't satisfy on-shell conditions. We assume that the component proportional to the proton momentum p is large compared to other components. Then we perform Taylor expansion for $S_1, ij(k)$ and $S_{2\alpha,ij}(k1, k2)$ around $k = (k \cdot n)p$ that can be expanded as follows:

$$k_i^\alpha = (k_i \cdot n)p^\alpha + (k_i \cdot p)n^\alpha + k_{i\perp}^\alpha = (k_i \cdot n)p^\alpha + \omega^\alpha_\beta k_i^\beta, \tag{2.6}$$

where $\omega^\alpha_\beta = g^\alpha_\beta - p^\alpha n_\beta$ and n is a lightlike vector which satisfies $n^2 = 0$ and $p \cdot n = 1$. We assume that the component propotional to p is much larger than other components here. Thus we perform Taylor expansion for $S_{1\,ji}(k), S^{a,\alpha}_{2ji,j'i'}(k_1, k_2)$ around $k_i = (k_i \cdot n)p$(collinear expansion) as

$$\begin{aligned}
& S_{1\,ji}(k) \\
= \; & S_{1\,ji}((k \cdot n)p) + \frac{\partial}{\partial k^\alpha} S_{1\,ji}(k)|_{k=(k\cdot n)p}\,(k - (k \cdot n)p)^\alpha + \cdots, \\
& S^{a,\alpha}_{2ji,j'i'}(k_1, k_2) \\
= \; & S^{a,\alpha}_{2ji,j'i'}((k_1 \cdot n)p, (k_2 \cdot n)p) + \frac{\partial}{\partial {k_1}^\alpha} S^{a,\alpha}_{2ji,j'i'}(k_1, k_2)|_{k_i=(k_i\cdot n)p} \\
& (k_1 - (k_1 \cdot n)p)^\alpha + \frac{\partial}{\partial {k_2}^\alpha} S^{a,\alpha}_{2ji,j'i'}(k_1, k_2)|_{k_i=(k_i\cdot n)p}(k_2 - (k_2 \cdot n)p)^\alpha + \cdots.
\end{aligned} \tag{2.7}$$

One can show $(k_i - (k_i \cdot n)p)^\alpha = \omega^\alpha_\beta k_i^\beta$. The leading contribution from the first diagram in FIG 2.1 in the collinear expansion is given by

$$\begin{aligned} & \int \frac{d^4k}{(2\pi)^4} S_{1,ji}(k) M_{1ij}(k) \\ = & \int \frac{d^2k_\perp}{(2\pi)^2} \int \frac{dk^+}{2\pi} \frac{dk^-}{2\pi} \int d^4\xi e^{ik\cdot\xi} \langle p|\bar{\psi}_j(0)\psi_i(\xi)|p\rangle S_{1ji}((k\cdot n)p), \end{aligned} \tag{2.8}$$

where

$$\begin{aligned} d^4k &= dk^+dk^-d^2k_\perp = d(k\cdot p)d(k\cdot n)d^2k_\perp, \\ e^{ik\cdot\xi} &= \exp[i((k\cdot p)(\xi\cdot n) + (\xi\cdot p)(k\cdot n) - k_\perp\cdot\xi_\perp)]. \end{aligned} \tag{2.9}$$

Then the integrals receive the contribution from the proton matrix on the lightcone as

$$\begin{aligned} \int \frac{d^4k}{(2\pi)^4} S_{1,ji}(k) M_{1ij}(k) &= \int \frac{d(k\cdot n)}{2\pi} \frac{d(k\cdot p)}{2\pi} \int \frac{d^2{}_\perp}{(2\pi)^2} e^{ik\cdot\xi} \\ &= \int dx \int \frac{d\lambda}{2\pi} e^{i\lambda x} \langle p|\bar{\psi}_j(0)\psi_i(\lambda n)|p\rangle S_{1ji}(xp). \end{aligned} \tag{2.10}$$

The second diagram in FIG 2.1 can be calculated in the same way:

$$\begin{aligned} & \int \frac{d^4k_1}{(2\pi)^4} \int \frac{d^4k_2}{(2\pi)^4} \int d^4\xi_1 e^{ik_1\cdot\xi_1} \int d^4\xi_2 e^{i(k_2-k_1)\cdot\xi_2} \langle p|\bar{\psi}_j(0) g A^a_\alpha(\xi_2)\psi_i(\xi_1)|p\rangle S^{a,\alpha}_{2,ij,i'j'} \\ = & \int dx_1 dx_2 \int \frac{d\lambda}{2\pi} \frac{d\mu}{2\pi} e^{i\lambda x_1} e^{i\mu(x_2-x_1)} \langle p|\bar{\psi}_{jj'}(0) g A^a_\alpha(\mu n)\psi_{ii'}(\lambda n)|p\rangle S^{a,\alpha}_{2,ij,i'j'}(x_1 p, x_2 p). \end{aligned} \tag{2.11}$$

We also carry out the power counting in the proton matrix element part. We decompose the gauge field A^a_α into the component proportional to p and other components as

$$A^a_\alpha = \left(\omega^\beta_\alpha + p_\alpha n^\beta\right) A^a_\beta = \omega^\beta_\alpha A^a_\beta + p_\alpha n\cdot A^a. \tag{2.12}$$

The Ward-Takahashi identity Eq.(2.5) can be rewritten in the collinear limit as

$$\begin{aligned} & (k_2-k_1)_\alpha S^{a,\alpha}_{2ji,j'i'}(k_1,k_2) \\ = \; & (k_2\cdot n - k_1\cdot n)p_\alpha S^{a,\alpha}_{2ji,j'i'}(k_1,k_2) + \omega^\beta_\alpha (k_2-k_1)_\beta S^{a,\alpha}_{2ji,j'i'}(k_1,k_2) \\ = \; & (S_{1\,ji}(k_2) - S_{1\,ji}(k_1))(\mathrm{T}^a)_{i'j'}, \end{aligned} \tag{2.13}$$

We here ignore the subleading component ω^β_α. Then the contribution from the second diagram gives

$$\begin{aligned} & \int dx_1 dx_2 \int \frac{d\lambda}{2\pi}\frac{d\mu}{2\pi} e^{i\lambda x_1} e^{i\mu(x_2-x_1)} \langle p|\bar\psi_{jj'}(0) g n_\beta A^{a,\beta}(\mu n)\psi_{ii'}(\lambda n)|p\rangle p_\alpha S^{a,\alpha}_{2,ij,i'j'}(k_1,k_2) \\ = \; & \int dx_1 dx_2 \int \frac{d\lambda}{2\pi}\frac{d\mu}{2\pi} e^{i\lambda x_1} e^{i\mu(x_2-x_1)} \\ & \langle p|\bar\psi_{jj'}(0) g n_\beta A^{a,\beta}(\mu n)\psi_{ii'}(\lambda n)|p\rangle \frac{S_{1\,ji}(x_2 p) - S_{1,ji}(x_1 p)}{x_2 - x_1 - i\epsilon}(\mathrm{T}^a)_{i'j'}. \end{aligned}$$

The sign of the $i\epsilon$ is determined by the fact that the gluon line in the second diagram only couples with the final state quark line. We use the integral representation of the step function

$$\int dx \frac{1}{x-i\epsilon} e^{i\alpha x} = 2\pi i\theta(\alpha). \tag{2.14}$$

The second diagram finally reads

$$\int dx \int \frac{d\lambda}{2\pi} e^{i\lambda x} \langle p|\bar\psi_{jj'}(0) i g n_\beta A^{a,\beta}(\mu n)(\mathrm{T}^a)_{j'i'}\psi_{ii'}(\lambda n)|p\rangle S_{1,ji}(xp). \tag{2.15}$$

We combine the leading contributions from the first diagram Eq.(2.10) and the second diagram Eq.(2.15) as

$$\int dx \int \frac{d\lambda}{2\pi} e^{i\lambda x} \langle p|\bar\psi_j(0)\left(1 + i g n_\beta A^{a,\beta}(\mu n)(\mathrm{T}^a)_{i'j'}\right)\psi_i(\lambda n)|p\rangle S_{1\,ji}(xp). \tag{2.16}$$

Adding the leading contributions from more gluon-linked diagrams, one can construct the gauge-link operator which guarantees the gauge-invariance of a nonlocal operator.

$$\begin{aligned} & \mathrm{P}\exp\left(ig\int_{\lambda}^{0} d\mu n_{\beta} A^{a,\beta}(\mu n)(\mathrm{T}^{a})\right)_{i'j'} \\ = \;& 1 + g n_{\beta} A^{a,\beta}(\mu n)(\mathrm{T}^{a})_{i'j'} + \cdots, \end{aligned} \tag{2.17}$$

Finally we obtain the leading power contribution form the collinear expansion as

$$\begin{aligned} & \int \frac{d^4k_1}{(2\pi)^4} \int \frac{d^4k_2}{(2\pi)^4} S^{a,\alpha}_{2,ij,i'j'}(k_1,k_2) M^{a}_{2,\alpha,ij,i'j'}(k_1,k_2) \\ = \;& \int dx \int \frac{d\lambda}{2\pi} e^{i\lambda x} \langle p|\bar{\psi}_j(0)\,[0,\lambda]\,\psi_i(\lambda n)|p\rangle S_{1\,ji}(xp), \end{aligned} \tag{2.18}$$

where $[0,\lambda]$ is a shorthand notation of the gauge-link.

2.2 Definition of Twist

We define the meaning of 'twist' in this paper by means of the power-counting for the expansion of the proton matrix element[30]. We expand matrix elements in terms of the following vectors.

$$\begin{aligned} p^2 &= n^2 = 0, p\cdot n = 1, \dim[p] = 1, \dim[n] = -1, \\ S^{\alpha} &= S^{\alpha}_{\parallel} + M_N S^{\alpha}_{\perp}, p\cdot S = n\cdot S = 0, \dim[S_{\parallel}] = 1, \dim[S_{\perp}] = 0. \end{aligned} \tag{2.19}$$

where $\dim[\cdots]$ denotes the dimension of mass. We work in hadron frame[31] at collinear limit and the kinematics aforementioned are shown in FIG 2.3. The exact expressions defined before can be constructed as

$$q^{\mu} = (0,0,0,-Q)\,, x_{bj} = \frac{Q^2}{2p\cdot q}, p^{\mu} = \frac{Q}{2x_b}(1,0,0,1)\,, n^{\mu} = \frac{x_b}{Q}(1,0,0,-1). \tag{2.20}$$

We use p, P_h denote the ingoing and outgoing momentum, other parameters can be derived revolved around the given variables. As p_{out} is on shell that satisfies

$$p'^2 = m^2, \tag{2.21}$$

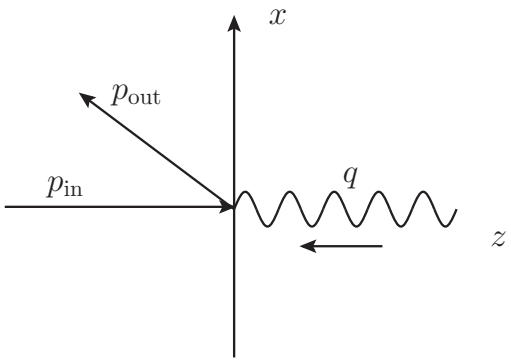

FIG 2.3 Hadron frame .

one can construct p'^{μ} like

$$P_h^{\mu} = \frac{z_f Q}{2}(1 + \frac{q_T^2}{Q^2} + \frac{m^2}{z_f^2 Q^2}, \frac{2q_T}{Q}, 0, -1 + \frac{q_T^2}{Q^2} + \frac{m^2}{z_f^2 Q^2}). \tag{2.22}$$

where q_T defined in Eq(2.23) describes transverse momentum from parton which is not zero in general

$$q_T^{\mu} = q^{\mu} + \frac{m^2 q_T \cdot q}{(p \cdot p')^2} p^{\mu} - \frac{p' \cdot q}{p \cdot p'} p^{\mu} - \frac{p \cdot q}{p \cdot p'} p'^{\mu}, \tag{2.23}$$

that is constrained by

$$q_T \cdot P_h = q_T \cdot p = 0. \tag{2.24}$$

One can expand a proton matrix element in terms of the variables as

$$\int \frac{d\lambda}{2\pi} e^{i\lambda x} \langle p|\bar{\psi}_j(0)\psi_i(\lambda n)|p\rangle \quad = \quad \frac{f_2}{2}(\lambda)(\not{p})_{ij} + M f_3(\lambda)\delta_{ij} + M^2 f_4(\lambda)(\not{n})_{ij}. \tag{2.25}$$

The nucleon mass M_N was introduced in order to make all the nonperturbative functions dimensionless. The function f_t with the coefficient M_N^{t-2} contribute to a cross section in the form of

$$\left(\frac{M_N}{Q}\right)^{t-2} f_t, \tag{2.26}$$

where Q is a typical energy scale of a process. We call this function 'twist-t function'. In a hard process, higher twist functions are suppressed by the large scale Q. Substituting the twist-2 function in (2.25) into (2.18), we can show

$$\frac{1}{2}\int \frac{dx}{x} f(x)\mathrm{Tr}\left[x\not{p}\gamma^{\mu}(\not{p}+\not{q})\gamma^{\nu}\right]\delta(xp+q)^2 . \tag{2.27}$$

One can show that this gives the Callan-Gross relation predicted by the parton model. We find that the collinear expansion can correctly reproduce the conventional result.

2.3 Twist-3 Calculation

The leading contribution to the SSA arises from the twist-3 function. One can find that the twist-3 effect from the first diagram in FIG2.1 is given by the subleading term in the collinear expansion (2.7)

$$\int \frac{d^4k}{(2\pi)^4}\int d^4\xi\, e^{ik\cdot\xi}\langle p|\bar{\psi}_j(0)\psi_i(\xi)|p\rangle \frac{\partial}{\partial k^{\alpha}} S_{1,ji}(k)|_{k=(k\cdot n)p}\omega^{\alpha}{}_{\beta}k^{\beta}, \tag{2.28}$$

Through the integration by part we find

$$\begin{aligned}&\int \frac{d^4k}{(2\pi)^4}\int d^4\xi\, e^{ik\cdot\xi}\langle p|\bar{\psi}_j(0)\psi_i(\xi)|p\rangle \frac{\partial}{\partial k^{\alpha}} S_{1,ji}(k)|_{k=(k\cdot n)p}\omega^{\alpha}{}_{\beta}k^{\beta}\\ =\;& i\omega^{\alpha}{}_{\beta}\int dx\int \frac{d\lambda}{2\pi}\, e^{i\lambda x}\langle p|\bar{\psi}_j(0)\partial^{\beta}\psi_i(\xi)|p\rangle \frac{\partial}{\partial k^{\alpha}} S_{1,ji}(k)|_{k=xp},\end{aligned} \tag{2.29}$$

One can check that Eq. (2.29) does not take a gauge invariant form without taking other terms into the consideration. There are two same power contributions from the second diagram in FIG2.1, [the subleading term in the collinear expansion + the leading term in the gauge field] and [the leading term in the collinear expansion + the subleading term in the gauge field] in and (2.12) and (2.7),

$$\begin{aligned}&\int \frac{d^4k_1}{(2\pi)^4}\frac{d^4k_2}{(2\pi)^4}\int d^4\xi_1\, e^{ik_1\cdot\xi_1} d^4\xi_2 e^{i(k_2-k_1)\cdot\xi_2}\Big[\langle p|\bar{\psi}_{jj'}(0)gA^a_{\alpha}(\xi_2)\psi_{ii'}(\xi_1)|p\rangle\omega^{\alpha}{}_{\beta}\\ &S^{a,\beta}_{2ji,j'i'}(k_1\cdot n,k_2\cdot n)+\langle p|\bar{\psi}_{jj'}(0)gn^{\sigma}A^a_{\sigma}(\xi_2)\psi_{ii'}(\xi_1)|p\rangle p_{\alpha}\Big(\frac{\partial}{\partial k_1^{\rho}}S^{a,\alpha}_{2ji,j'i'}|_{k_i=x_ip}\,\omega^{\rho}{}_{\beta}k_1^{\beta}\\ &+\frac{\partial}{\partial k_2^{\rho}}S^{a,\alpha}_{2ji,j'i'}|_{k_i=x_ip}\,\omega^{\rho}{}_{\beta}k_2^{\beta}\Big)\Big].\end{aligned} \tag{2.30}$$

We take derivatives of $S^{a,\alpha}_{2,ji,j'i'}$ with respect to k_1 and k_2 as

$$
\begin{aligned}
p_\alpha \frac{\partial}{\partial k_2^\rho} S^{a,\alpha}_{2,ji,j'i'}|_{k_i=x_i p} &= \frac{-1}{k_2\cdot n - k_1\cdot n - i\epsilon}\Big[S^{a,\rho}_{2,ji,j'i'}(k_1\cdot n, k_2\cdot n) - \frac{\partial}{\partial k_2^\rho} S_{1,ji}(k_2)|_{k_2=(k_2\cdot n)p}(\mathrm{T}^a)_{j'i'}\Big] \\
p_\alpha \frac{\partial}{\partial k_1^\rho} S^{a,\alpha}_{2,ji,j'i'}|_{k_i=x_i p} &= \frac{1}{k_2\cdot n - k_1\cdot n - i\epsilon}\Big[S^{a,\rho}_{2,ji,j'i'}(k_1\cdot n, k_2\cdot n) - \frac{\partial}{\partial k_1^\rho} S_{1,ji}(k_1)|_{k_1=(k_1\cdot n)p}(\mathrm{T}^a)_{j'i'}\Big].
\end{aligned}
$$

We substitute these relations into the second term in (2.30),

$$
\begin{aligned}
&\langle p|\bar\psi_{jj'}(0) g n^\sigma A^a_\sigma(\xi_2)\psi_{ii'}(\xi_1)|p\rangle p_\alpha\Big(\frac{\partial}{\partial k_1^\rho} S^{a,\alpha}_{2,ji,j'i'}|_{k_i=x_i p}\,\omega^\rho{}_\beta k_1^\beta + \frac{\partial}{\partial k_2^\rho} S^{a,\alpha}_{2,ji,j'i'}|_{k_i=x_i p}\,\omega^\rho{}_\beta k_2^\beta\Big) \\
= &\int \frac{d^4k_1}{(2\pi)^4}\frac{d^4k_2}{(2\pi)^4}\int d^4\xi_1 e^{ik_1\cdot\xi_1} d^4\xi_2 e^{i(k_2-k_1)\cdot\xi_2}\langle p|\bar\psi_{jj'}(0) g n^\sigma A^a_\sigma(\xi_2)\psi_{ii'}(\xi_1)|p\rangle \\
&\times\Big[\Big(-\frac{1}{k_2\cdot n - k_1\cdot n - i\epsilon} S^{a,\rho}_{2,ji,j'i'}(k_1\cdot n, k_2\cdot n) + \frac{\partial}{\partial k_2^\rho} S_{1,ji}(k_2)|_{k_2=(k_2\cdot n)p}(\mathrm{T}^a)_{j'i'}\Big) \\
&\omega^\rho{}_\beta (k_2-k_1)^\beta + \Big(\frac{\partial}{\partial k_2^\rho} S_{1,ji}(k_2)|_{k_2=(k_2\cdot n)p}(\mathrm{T}^a)_{j'i'} - \frac{\partial}{\partial k_1^\rho} S_{1,ji}(k_1)|_{k_1=(k_1\cdot n)p}(\mathrm{T}^a)_{j'i'}\Big)\omega^\rho{}_\beta k_1^\beta\Big]
\end{aligned}
\tag{2.31}
$$

One can perform the integration by part following the same procedure with Eq. (2.29) and use the integral representation of the step function for the last term,

$$
\begin{aligned}
&\int dx_1 dx_2 \int \frac{d\lambda}{2\pi}\frac{d\mu}{2\pi} e^{i\lambda x_1} e^{i\mu(x_2-x_1)}\omega^\rho{}_\beta \langle p|\bar\psi_{jj'}(0) g n^\sigma \partial^\beta A^a_\sigma(\mu n)\psi_{ii'}(\lambda n)|p\rangle \\
&\frac{-iS^a_{2\rho,ji,j'i'}(x_1 p, x_2 p)}{x_2 - x_1 - i\epsilon} + \int dx_1 dx_2 \int \frac{d\lambda}{2\pi}\frac{d\mu}{2\pi} e^{i\lambda x_1} e^{i\mu(x_2-x_1)}\langle p|\bar\psi_j(0) g n^\sigma n^\sigma \\
&\partial^\beta A_\sigma(\mu n)\psi_i(\lambda n)|p\rangle i\omega^\rho{}_\beta \frac{1}{x_2 - x_1 - i\epsilon}\frac{\partial S_{1,ji}(k_2)}{\partial k_2^\rho}|_{k_2=x_2 p} \\
&+ \int dx \int \frac{d\lambda}{2\pi} e^{i\lambda x}\langle p|\bar\psi_j(0) i g n^\sigma \int_\lambda^0 d\mu\, n^\sigma A_\sigma(\mu n)\partial^\beta\psi_i(\lambda n)|p\rangle i\omega^\rho{}_\beta \frac{\partial S_{1,ji}(k)}{\partial k^\rho}|_{k=xp}.
\end{aligned}
\tag{2.32}
$$

For the first and the second terms, we construct the field strength tensor of gluon

$$
\partial^\beta A^a_\sigma(\mu n) = F^{\beta a}_{\ \ \sigma}(\mu n) + n^\sigma \partial_\sigma A^a_\beta(\mu n), \tag{2.33}
$$

where we ignored the nonlinear term of the gluon fields because it is given by the more gluon-linked diagram. Thus the first and the second terms in (2.32) can be calculated as

$$\begin{aligned}
&\int dx_1 dx_2 \int \frac{d\lambda}{2\pi}\frac{d\mu}{2\pi} e^{i\lambda x_1} e^{i\mu(x_2-x_1)} \omega^{\rho}_{\ \beta} \langle p|\bar{\psi}_{jj'}(0) g n^{\sigma} F^{a\beta}_{\ \ \sigma}(\mu n)\psi_{ii'}(\lambda n)|p\rangle \\
&\frac{-iS^{a}_{2\rho,ji,j'i'}(x_1 p, x_2 p)}{x_2 - x_1 - i\epsilon} + \int dx \int \frac{d\lambda}{2\pi} e^{i\lambda x} \langle p|\bar{\psi}_j(0) ig \int_{\lambda}^{\infty} d\mu\, n^{\sigma} F^{\beta}_{\ \ \sigma}(\mu n)\psi_i(\lambda n)|p\rangle \\
&i\omega^{\rho}_{\ \beta} \frac{\partial S_{1,ji}(k)}{\partial k^{\rho}}|_{k=xp} + i\int dx \int \frac{d\lambda}{2\pi} e^{i\lambda x} \langle p|\bar{\psi}_j(0)(-igA^{\beta}(\mu n)\psi_i(\lambda n)|p\rangle i\omega^{\rho}_{\ \beta} \frac{\partial S_{1,ji}(k)}{\partial k^{\rho}}|_{k=xp} \\
&- \int dx_1 dx_2 \int \frac{d\lambda}{2\pi}\frac{d\mu}{2\pi} e^{i\lambda x_1} e^{i\mu(x_2-x_1)} \langle p|\bar{\psi}_{jj'}(0) g A^{a}_{\alpha}(\mu n)\psi_{ii'}(\lambda n)|p\rangle \omega^{\alpha}_{\ \beta} S^{a,\beta}_{2,ji,j'i'}(x_1 p, x_2 p).
\end{aligned} \tag{2.34}$$

The last term is canceled with the first term in (2.30). Combining all terms in (2.29), (2.32) and (2.34), we can obtain the formula for the twist-3 contribution with gauge-invariant proton matrices.

$$\begin{aligned}
W^{\mu\nu}_{\text{twist}-3} &= i\omega^{\rho}_{\ \beta} \int dx M^{\beta}_{\partial,ij} \frac{\partial}{\partial k^{\rho}} S^{\mu\nu}_{1\,ji}(k)|_{k=xp} \\
&\quad -i\omega^{\rho}_{\ \beta} \int dx_1 dx_2 M^{a\beta}_{,F,ij,i'j'} \frac{1}{x_2 - x_1 - i\epsilon} S^{a\,\mu\nu}_{2\rho,ji,j'i'}|_{x_i p},
\end{aligned} \tag{2.35}$$

where

$$\begin{aligned}
M^{\beta}_{\partial,ij} &= \int \frac{d\lambda}{2\pi} e^{i\lambda x} \langle p|\bar{\psi}_j(0)\,[0,\infty]\,\partial^{\beta}([\infty,\lambda n]\,\psi_i(\lambda n))|p\rangle \\
&= \int \frac{d\lambda}{2\pi} e^{i\lambda x} \langle p|\bar{\psi}_j(0)\,[0,\lambda n]\,D^{\beta}(\lambda n)\psi_i(\lambda n))|p\rangle \\
&\quad + \int \frac{d\lambda}{2\pi} e^{i\lambda x} \int_{\lambda}^{\infty} d\mu \langle p|\bar{\psi}_j(0)\,[0,\mu n]\,ig n^{\sigma} F^{\beta}_{\ \ \sigma}(\mu n)\,[\mu n,\lambda n]\,\psi_i(\lambda n)|p\rangle, \\
M^{a\beta}_{Fij,i'j'} &= \int \frac{d\lambda}{2\pi}\frac{d\mu}{2\pi} e^{i\lambda x_1} e^{i\mu(x_2-x_1)} \langle p|\bar{\psi}_{jj'}(0)\,[0,\mu n]\,g n^{\sigma} F^{a\beta}_{\ \ \sigma}(\mu n)\,[\mu n,\lambda n]\,\psi_{ii'}(\lambda n)|p\rangle,
\end{aligned} \tag{2.36}$$

and the Lorentz indices of the photon lines μ, ν were restored. So far we have shown the detailed calculation of differential cross section up to twist-3 level in the quark case. One can drive the corresponding formula for the gluon Sivers effect in the same way [32]. We just show the result here because the calculation is much more complicated than the quark

case.

$$W^{\mu\nu}_{\text{twist}-3} = \omega^{\mu}_{\alpha}\omega^{\nu}_{\beta}\omega^{\lambda}_{\gamma}\int\frac{dx}{x^2}\Phi^{\alpha\beta\gamma}_{\partial}\frac{\partial}{\partial k^{\lambda}}S_{\mu\nu,\rho\sigma}|_{k=xp} - \frac{1}{2}\omega^{\mu}_{\alpha}\omega^{\nu}_{\beta}\omega^{\lambda}_{\gamma} \frac{1}{x_1 - i\epsilon}\frac{1}{x_2 + i\epsilon}\frac{1}{x_2 - x_1 - i\epsilon}\int dx_1 dx_2 M^{\alpha\beta\gamma}_{F,abc}S^{abc}_{\mu\nu\lambda,\rho\sigma}. \quad (2.37)$$

We will use this formula in our study on the SSA in the J/ψ production.

Chapter 3 Twist-3 Gluon Contribution in J/ψ Productions

In this chapter we perform calculations for J/ψ productions in color-singlet model following NRQCD and formalism illustrated above.

3.1 Non-Relativistic QCD

The NRQCD factorization mechanism is widely applied in heavy quarkonium productions[33–35] in which a cross section reads

$$d\sigma_H = \sum_n \sigma_{q\bar{q}[n]} \langle O[n] \rangle_H , \tag{3.1}$$

where $\sigma_H, \sigma_{q\bar{q}}[n]$ denotes the hard cross section and the creations of the quark pair with Fock states respectively , $\langle O[n] \rangle_H$ is the long distance matrix element(LDME) that describes the corresponding quark pair $q\bar{q}$ hadronlizing into final quarkonium H. LDME is universal and n denotes possible Fock states for final quarkonium

$$n = ^{2s+1} L_j^c. \tag{3.2}$$

where s, j, L, c stand for spin,total angular momentum,OAM and color state shown as follows

$$n = ^3 S_1^{[1]}, ^1 S_1^{[8]}, ^3 S_1^{[8]} \cdots , \tag{3.3}$$

In this thesis we concentrate on the color-singlet channel $^3S_1^{[1]}$ where specific diagrams for hard scattering are shown in FIG 3.1. The relevant amplitude $\mathcal{M}$ in singlet state is given by[**?**]

$$\mathcal{M}\left[^3 S_1^{[1]}\right] = \epsilon_\alpha \mathrm{Tr}\left[\mathcal{T} \Pi_1^\alpha C_{[1]}\right]|_{q=0}, \tag{3.4}$$

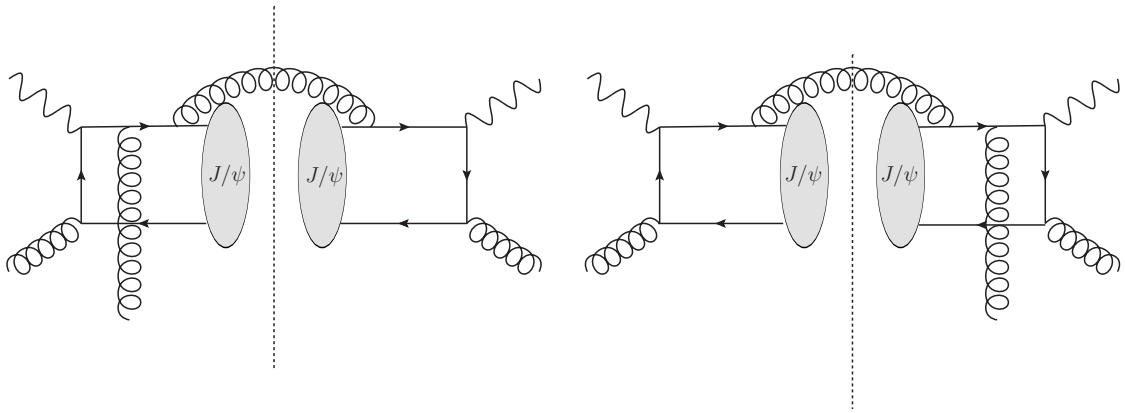

FIG 3.1 Diagrams for color-singlet J/ψ.

where $\mathcal{T}$ represents the scattering amplitudes shown in FIG 3.1 and Π_1^α denotes the projector on color-singlet state given by

$$\Pi_1^\alpha = \frac{1}{\sqrt{8m^3}}(\not{p} - \not{q} - m)\gamma^\alpha(\not{p} + \not{q} + m), \tag{3.5}$$

The ϵ_α in Eq. (3.4) represents the polarization vector that satisfies

$$\sum \epsilon_\alpha \epsilon_\beta^* = -g_{\alpha\beta} + \frac{p_\alpha p_\beta}{m^2}, \tag{3.6}$$

and $C_{[1]}$ is the relevant parameter as

$$C_{[1]} = \frac{1}{\sqrt{3}}\mathbf{1}. \tag{3.7}$$

We will deal with the hadronization effect of J/ψ based on this framework.

3.2 Kinematics

In this thesis we work in hadron frame and the full picture of scattering can be represented as FIG 3.2. One can define a set of Lorentz invariant variables like

$$\begin{aligned} S_{ep} &= (p+\ell)^2, Q^2 = -q^2 = -(\ell - \ell')^2, x_B = \frac{Q^2}{2p\cdot q}, \\ z_f &= \frac{p\cdot P_{J/\psi}}{p\cdot q}, S_\perp = (0, \cos\Phi_s, \sin\Phi_s, 0), \end{aligned} \tag{3.8}$$

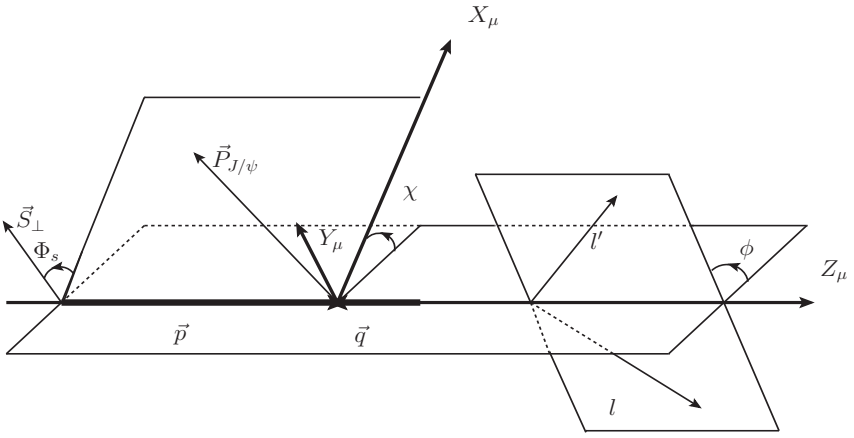

FIG 3.2 Full picture for scattering in hadron frame.

where S_{ep} stands for the total energy of scatterings, Q^2 represents the energy transfer, x_B is the fixed Bjorken scaling variable, z_f gives the fraction of parent proton's momentum carried by final parton and $S_\perp$ is the transversely polarized spin. The partonic scattering can be described by specific diagrams as FIG 3.3 in terms of the variables aforementioned.

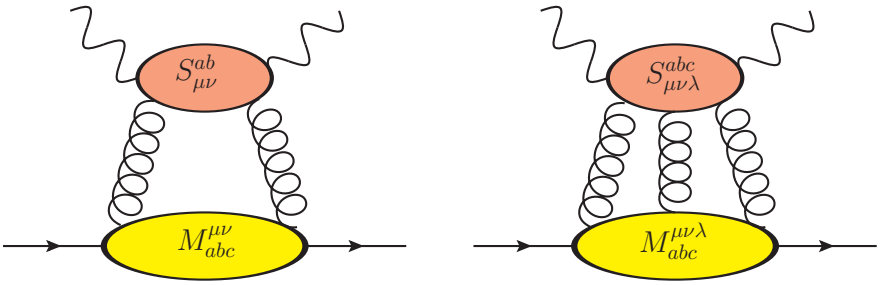

FIG 3.3 Partonic scattering, the first denotes the unpolarized scattering and the later one polarized.

From the perspective of Lorentz invariance, the hadronic tensor can be decomposed in terms of nine symmetry tensors given by[31]

$$W^{\mu\nu} = \sum_{k=1}^{9} W^{\rho\sigma} \tilde{V}_{k\rho\sigma} V_k^{\mu\nu}, \tag{3.9}$$

where $V_k^{\mu\nu}$, $\tilde{V}_{k\rho\sigma}$ are constrained as

$$\tilde{V}_{k\rho\sigma} V_{k'}^{\rho\sigma} = \delta_{kk'}, \tag{3.10}$$

Here we just show the explicit definitions of the symmetric tensors that are relevant to our study.

$$\mathcal{V}_1^{\mu\nu} = X^\mu X^\nu + Y^\mu Y^\nu, \quad \mathcal{V}_2^{\mu\nu} = g^{\mu\nu} + Z^\mu Z^\nu, \quad \mathcal{V}_3^{\mu\nu} = T^\mu X^\nu + X^\mu T^\nu,$$
$$\mathcal{V}_4^{\mu\nu} = X^\mu X^\nu - Y^\mu Y^\nu, \quad \mathcal{V}_8^{\mu\nu} = T^\mu Y^\nu + Y^\mu T^\nu, \quad \mathcal{V}_9^{\mu\nu} = X^\mu Y^\nu + Y^\mu X^\nu,$$

$$\widetilde{\mathcal{V}}_1^{\mu\nu} = \frac{1}{2}(2T^\mu T^\nu + X^\mu X^\nu + Y^\mu Y^\nu), \quad \widetilde{\mathcal{V}}_2^{\mu\nu} = T^\mu T^\nu, \quad \widetilde{\mathcal{V}}_3^{\mu\nu} = -\frac{1}{2}(T^\mu X^\nu + X^\mu T^\nu),$$
$$\widetilde{\mathcal{V}}_4^{\mu\nu} = \frac{1}{2}(X^\mu X^\nu - Y^\mu Y^\nu), \quad \widetilde{\mathcal{V}}_8^{\mu\nu} = -\frac{1}{2}(T^\mu Y^\nu + Y^\mu T^\nu), \quad \widetilde{\mathcal{V}}_9^{\mu\nu} = \frac{1}{2}(X^\mu Y^\nu + Y^\mu X^\nu),$$

where the four vectors are given by

$$\begin{aligned} T^\mu &= (1,0,0,0), X^\mu = (0,\cos\chi,\sin\chi,0), \\ Y^\mu &= (0,-\sin\chi,\cos\chi,0), Z^\mu = (0,0,0,1). \end{aligned} \tag{3.11}$$

The calculation of $L_{\mu\nu}W^{\mu\nu}$ can be evaluated as follows in terms of these vectors aforementioned.

$$L_{\mu\nu}W^{\mu\nu} = \sum_{i=1,\cdots,4,8,9} [L_{\mu\nu}\mathcal{V}_i^{\mu\nu}][W_{\rho\sigma}\widetilde{\mathcal{V}}_i^{\rho\sigma}] = Q^2 \sum_{i=1,\cdots,4,8,9} \mathcal{A}_i(\phi-\chi)[W_{\rho\sigma}\widetilde{\mathcal{V}}_i^{\rho\sigma}]. \tag{3.12}$$

These azimuthal dependences $\mathcal{A}_i(\varphi)$ are given by[36] ,

$$\begin{aligned} \mathcal{A}_1(\varphi) &= \frac{4}{y^2}\Big(1-y+\frac{y^2}{2}\Big), \mathcal{A}_2(\varphi) = -2, \\ \mathcal{A}_3(\varphi) &= -\frac{4}{y^2}(2-y)\sqrt{1-y}\cos\varphi, \mathcal{A}_4(\varphi) = \frac{4}{y^2}(1-y)\cos 2\varphi, \\ \mathcal{A}_8(\varphi) &= -\frac{4}{y^2}(2-y)\sqrt{1-y}\sin\varphi, \mathcal{A}_9(\varphi) = \frac{4}{y^2}(1-y)\sin 2\varphi. \end{aligned} \tag{3.13}$$

symbol y denotes $y = \dfrac{Q^2}{x_b S_{ep}}$.

3.3 Twist-2 Contribution in Color-Singlet J/ψ Productions

Following the similar procedure in quark case, we perform the calculation for twist-2 case in the first place. The Feynman diagrams contribute to the twist-2, or equiva-

lently, the unpolarized contributions in color-singlet channel can be represented as follows. Adopting the assumption of NRQCD that the color-singlet production takes the

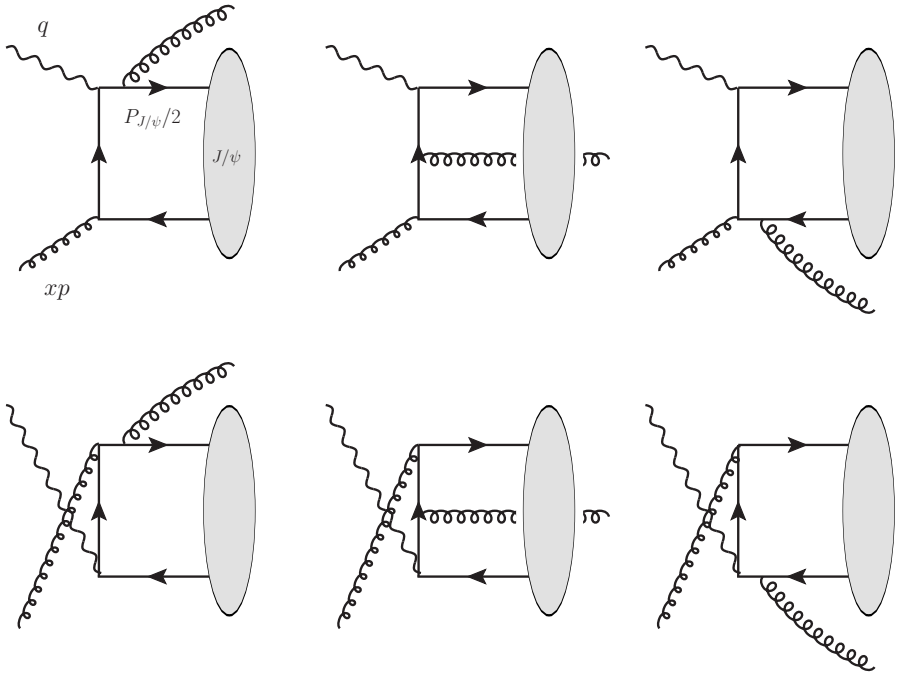

FIG 3.4 Feynman diagrams contribute to unpolarized/twist-2 cross sections.

majority and we ignore the color-octet case. Thus we consider the projector on color-singlet state only. The unpolarized amplitude of the scattering is given by

$$W^{\mu\nu}(p,q,P_{J/\psi}) = \int_0^1 \frac{dx}{x} G(x) \langle O^{J/\psi}(^3S_1^{[1]})\rangle \, w^{\mu\nu}(xp,q,P_{J/\psi}), \tag{3.14}$$

Combining with the leptonic tensor, one can derive the differential cross section formula for unpolarized(twist-2) as

$$\begin{aligned} &\frac{d^6\sigma^{\text{unpol}}}{dx_b dQ^2 dz_f dP_T^2 d\phi d\chi} \\ &= \frac{\alpha_{em}^2 \alpha_s^2 e_c^2}{4\pi S_{ep}^2 x_B^2 Q^2}\Big(\mathcal{N}\langle O^{J/\psi}(^3S_1^{[1]})\rangle\Big) \\ &\quad \sum_{i=1,\cdots,4,8,9} \mathcal{A}_i(\phi-\chi) \int_0^1 \frac{dx}{x} G(x)\, \hat{\sigma}_i\, \delta\Big[\frac{P_T^2}{Q^2} - \Big(1-\frac{1}{\hat{x}}+\frac{m_{J/\psi}^2}{z_f Q^2}\Big)\Big(1-\frac{1}{z_f}\Big)\Big]. \end{aligned} \tag{3.15}$$

where α_{em}, α_s are the coupling coefficient of the QCD and QED respectively, σ_i denote the hard cross sections whose exact expressions are listed in Appendix and $G(x)$ stands for the parton distribution function of gluons.

3.4 Twist-3 Contribution in Color-Singlet J/ψ Productions

We follow the similar procedure in quark case aforementioned that started from the Ward identity as

$$\begin{aligned} k\cdot nS_{p\nu}(k)+\omega_\kappa^\mu k^\kappa S_{\mu\nu}(k)=k\cdot nS_{\mu p}(k)+\omega_\kappa^\nu k^\kappa S_{\mu\nu} &= 0,\\ (k_2\cdot n-k_1\cdot n)S^{abc}_{\mu\nu p}(k_1,k_2)+\omega_\kappa^\lambda(k_2-k_1)^\kappa S^{abc}_{\mu\nu\lambda}(k_1,k_2) &= if^{abc}(S_{\mu\nu}(k_2)-S_{\mu\nu}(k_1)),\\ k_1\cdot nS^{abc}_{p\nu\lambda}(k_1,k_2)+\omega_\kappa^\lambda k_1^\kappa &= -if^{abc}S_{\mu\nu}(k_2),\\ k_2\cdot nS^{abc}_{p\nu\lambda}(k_1,k_2)+\omega_\kappa^\lambda k_2^\kappa &= -if^{abc}S_{\mu\nu}(k_1). \end{aligned} \tag{3.16}$$

Then we collect all terms securing the gauge invariance and calculate it through the Ward identity as

$$\begin{aligned} &W^{\text{hard part}}\\ =&\int\frac{d^4k}{(2\pi)^4}\int d^4\xi e^{ik\cdot\xi}\langle pS_\perp|A_b^\nu(0)A_a^\mu(\xi)|pS_\perp\rangle S^{ab}_{\mu\nu}(k)\\ &+\frac{1}{2}\int\frac{d^4k_1}{(2\pi)^4}\frac{d^4k_2}{(2\pi)^4}\int d^4\xi e^{ik_1\cdot\xi}d^4\eta e^{i\eta(k_2-k_1)}\langle pS_\perp|A_b^\nu(0)A_c^\lambda(\eta)A_a^\mu(\xi|pS_\perp\rangle S^{abc}_{\mu\nu\lambda}(k_1,k_2), \end{aligned} \tag{3.17}$$

The factor $\frac{1}{2}$ is induced according to the interchange symmetry. Thus the first term can be computed like

$$\begin{aligned} &\int\frac{d^4k}{(2\pi)^4}\int d^4\xi e^{ik\cdot\xi}\langle pS_\perp|A_b^\nu(0)A_a^\mu(\xi)|pS_\perp\rangle S^{ab}_{\mu\nu}(k)\\ =&\int\frac{d^4k}{(2\pi)^4}\frac{\omega_\delta^\nu\omega_\tau^\mu}{(k\cdot n)^2}\langle pS_\perp|A_b^\beta(0)A_a^\alpha(\xi)|pS_\perp\rangle(k\cdot ng_\alpha^\tau-n_\alpha k^\tau)(k\cdot ng_\beta^\delta-n_\beta k^\delta)S^{ab}_{\mu\nu}(k)\\ =&\int\frac{d^4k}{(2\pi)^4}\frac{\omega_\delta^\nu\omega_\tau^\mu}{(k\cdot n)^2}\langle pS_\perp|F_b^{\delta\beta}(0)F_a^{\tau\alpha}(\xi)|pS_\perp\rangle S^{ab}_{\mu\nu}, \end{aligned} \tag{3.18}$$

where the field tensor is given by

$$F_b^{\delta\beta}(0) \equiv \partial^\delta A_b^\beta(0) - \partial^\beta A_b^\delta(0), \tag{3.19}$$

relation below is essential in the calculation of Eq(3.18).

$$k_1^\iota n_\alpha - k_1 \cdot n g_\alpha^\iota = -i\Big(\frac{\partial}{\partial \xi_\iota} e^{ik_1\cdot\xi} n_\alpha - \frac{\partial}{\partial \xi_\delta} e^{ik_1\cdot\xi} n_\delta g_\alpha^\iota\Big). \tag{3.20}$$

Therefore one can perform the expansion of $S_{\mu\nu\lambda}^{abc}$ up to the first order as Eq(2.7) and obtain expressions for the first part in Eq(3.17) as follows.

$$\begin{aligned}
&\int \frac{d^4k}{(2\pi)^4} \int d^4\xi e^{ik\cdot\xi} \langle pS_\perp | A_b^\nu(0) A_a^\mu(\xi) | pS_\perp \rangle S_{\mu\nu}^{ab}(k) \\
= \;& \omega_\delta^\nu \omega_\tau^\mu \int \frac{dx}{x^2} \int \frac{d\lambda}{2\pi} e^{i\lambda x} \langle pS_\perp | F_b^{\delta\beta}(0) F_a^{\tau\alpha}(\xi) | pS_\perp \rangle S_{\mu\nu}^{ab}(xp) \\
& + i\omega_\delta^\nu \omega_\tau^\mu \omega_\theta^\zeta \int \frac{dx}{x^2} \int \frac{d\lambda}{2\pi} e^{i\lambda x} \langle pS_\perp | F_b^{\delta\beta}(0) \partial^\theta F_a^{\tau\alpha}(\xi) | pS_\perp \rangle \frac{\partial}{\partial k^\xi} S_{\mu\nu}^{ab}(xp).
\end{aligned} \tag{3.21}$$

The second part in Eq(3.17) can be compute in a similar approach and can obtain

$$\begin{aligned}
& \langle pS_\perp | A_b^\nu(0) A_c^\lambda(\eta) A_a^\mu(\xi) | pS_\perp \rangle S_{\mu\nu\lambda}^{abc}(k_1, k_2) \\
= \;& \langle pS_\perp | A_b^\beta(0) A_c^\gamma(\eta) A_a^\alpha(\xi) | pS_\perp \rangle (\omega_\alpha^\mu + p^\mu n_\alpha)(\omega_\beta^\nu + p^\nu n_\beta)(\omega_\gamma^\lambda + p^\lambda n_\gamma) S_{\mu\nu\lambda}^{abc}(k_1, k_2) \\
= \;& \langle pS_\perp | A_b^\beta(0) A_c^\gamma(\eta) A_a^\alpha(\xi) | pS_\perp \rangle \Big[-\frac{1}{x_1 - i\epsilon} \frac{1}{x_2 + i\epsilon} \frac{\omega_\iota^\mu \omega_\chi^\nu \omega_\eta^\lambda}{x_2 - x_1 - i\epsilon} (k_1^\iota n_\alpha - k_1 \cdot n g_\alpha^\iota) \\
& (k_2^\chi n_\beta - k_2 \cdot n g_\beta^\chi)((k_2 - k_1)^\eta n_\gamma - (k_2 \cdot n - k_1 \cdot n) g_\beta^\eta) S_{\mu\nu\lambda}^{abc}(k_1, k_2) + \frac{-if^{abc}}{x_1 - i\epsilon} \\
& \frac{n_\alpha}{(x_2 + i\epsilon)^2} \omega_\chi^\nu \omega_\eta^\lambda (k_2^\chi n_\beta - k_2 \cdot n g_\beta^\chi)(k_2^\eta n_\gamma - k_2 \cdot n g_\gamma^\eta) S_{\nu\lambda}(k_2) + \frac{-if^{abc}}{(x_1 - i\epsilon)^2} \\
& \frac{n_\beta}{x_2 + i\epsilon} \omega_\chi^\nu \omega_\eta^\lambda (k_1^\iota n_\alpha - k_1 \cdot n g_\alpha^\iota)(k_1^\eta n_\gamma - k_1 \cdot n g_\gamma^\eta) S_{\mu\lambda}(k_1) + \frac{if^{abc}}{x_1 - i\epsilon} \\
& \frac{1}{x_2 + i\epsilon} \frac{n_\gamma}{x_2 - x_1 - i\epsilon} \omega_\iota^\mu \omega_\chi^\nu (k_1^\iota n_\alpha - k_1 \cdot n g_\alpha^\iota)(k_2^\chi n_\beta - k_2 \cdot n g_\beta^\chi) S_{\mu\nu}(k_2) - \frac{if^{abc}}{x_1 - i\epsilon} \\
& \frac{1}{x_2 + i\epsilon} \frac{n_\gamma}{x_2 - x_1 - i\epsilon} \omega_\iota^\mu \omega_\chi^\nu (k_1^\iota n_\alpha - k_1 \cdot n g_\alpha^\iota)(k_2^\chi n_\beta - k_2 \cdot n g_\beta^\chi) S_{\mu\nu}(k_1) \Big],
\end{aligned} \tag{3.22}$$

One can treat Eq(3.22) in a similar approach as Eq(3.20). The first component of Eq(3.22) can be evaluated as

$$-\frac{1}{2}\omega_\iota^\mu\omega_\chi^\nu\omega_\eta^\lambda\int dx_1dx_2\int\frac{d\lambda}{2\pi}\frac{d\mu}{2\pi}e^{i\lambda x_1}e^{i\mu(x_2-x_1)}\langle pS_\perp|F_b^{\chi n}(0)F_c^{\eta n}(\mu n)F_a^{\iota n}(\lambda n)|pS_\perp\rangle$$
$$\frac{1}{x_1-i\epsilon}\frac{1}{x_2+i\epsilon}\frac{S^{abc}_{\mu\nu\lambda}(x_1p,x_2p)}{x_2-x_1-i\epsilon}. \tag{3.23}$$

The rest terms in Eq(3.22) can be computed in a comparable routine with one more theta integrations like

$$\lim_{\epsilon\to0^+}\frac{1}{2\pi i}\int_{-\infty}^{\infty}dx\frac{1}{x-i\epsilon}e^{ix\cdot t}=\theta(t), \tag{3.24}$$

We can get the final expressions for Eq(3.22) except for the first component shown as follows

$$\begin{aligned}&-if^{abc}\omega_\chi^\nu\omega_\eta^\lambda\int\frac{dx}{x^2}\int\frac{d\lambda}{2\pi}e^{i\lambda x}\Big[\langle pS_\perp|F_b^{\chi n}(0)ig\int_\lambda^0 d\mu A_a^n(\mu n)F_c^{\eta n}(\lambda n)|pS_\perp\rangle+\\&\langle pS_\perp|F_b^{\chi n}(0)igA_c^\eta(\lambda n)A_a^n(\lambda n)|pS_\perp\rangle+\langle pS_\perp|A_b^\chi(0)igA_c^n(0)F_a^{\eta n}(\lambda n)|pS_\perp\rangle\Big]S_{\nu\lambda}(xp),\\=\;&\omega_\chi^\nu\omega_\eta^\lambda\int\frac{dx}{x^2}\int\frac{d\lambda}{2\pi}e^{i\lambda x}\langle pS_\perp|F_b^{\chi n}(0)\,[0,\lambda n]_{bc}\,F_c^{\eta n}(\lambda n)|pS_\perp\rangle S_{\nu\lambda}(xp).\end{aligned} \tag{3.25}$$

Following the procedures aforementioned, we perform the Taylor expansions at collinear limit for the hard part and obtain the final gauge-invariant expression in gluon case up to twist-3 level as [32]

$$\begin{aligned}W_{\rho\sigma}\;=\;&+\omega_\chi^\nu\omega_\eta^\lambda\omega_\beta^\tau\int\frac{dx}{x^2}\Phi_\partial^{\chi\eta\beta}\frac{\partial}{\partial k^\tau}S_{\nu\lambda,\rho\sigma}|_{xp}\\&-\frac{1}{2}\omega_\chi^\nu\omega_\eta^\lambda\omega_\beta^\tau\frac{1}{x_1-i\epsilon}\frac{1}{x_2+i\epsilon}\frac{1}{x_2-x_1-i\epsilon}\int dx_1dx_2M_{F,abc}^{\chi\eta\beta}S^{abc}_{\nu\lambda\tau,\rho\sigma}.\end{aligned} \tag{3.26}$$

The $\Phi_{\partial}^{\alpha\beta\gamma}(x)$ denotes the kinematical functions and $M_{F,abc}^{\alpha\beta\gamma}$ stands for the dynamical functions shown as follows.

$$\begin{aligned}
\Phi_{\partial}^{\alpha\beta\gamma}(x) &= \int \frac{d\lambda}{2\pi} e^{i\lambda x} \langle pS_\perp | F^{\beta n}(0) F^{\alpha n}(\lambda n) | pS_\perp \rangle (i\overleftarrow{\partial}_\perp^{\gamma}), \\
\Phi^{\alpha\beta}(x) &= \int \frac{d\lambda}{2\pi} e^{i\lambda x} \langle pS_\perp | F^{\beta n}(0) F^{\alpha n}(\lambda n) | pS_\perp \rangle, \\
M_{F,abc}^{\alpha\beta\gamma} &= \int \frac{d\lambda}{2\pi} \frac{d\mu}{2\pi} e^{i\lambda x} e^{i\mu(x_2-x_1)} gi \langle pS_\perp | F_b^{\beta n}(0) F_c^{\gamma n}(\mu n) F_a^{\alpha n}(\lambda n) | pS_\perp \rangle. \quad (3.27)
\end{aligned}$$

One can discover that the expression is much complicated compared with the quark. It could be attributed to the complexity of pole structures appeared in gluon case. Besides, the freedom of color is also much complicated in gluon case. We perform the expansions for dynamical part with indexes *abc*. Work in SU(N) group we have the relation as

$$\mathrm{Tr}[F^a D^b] = 0, \mathrm{Tr}[F^a F^b] = N\delta^{ab}, \quad (3.28)$$

where $F^a \& D^b$ is short for $-if^{aef}$ and d^{bfe} respectively. One can perform the decomposition for $M_{F,abc}^{\alpha\beta\gamma}$ in terms of $if^{abc} \& d^{abc}$ as

$$M_{F,abc}^{\alpha\beta\gamma}(x_1, x_2) = \frac{-if^{abc}}{N(N^2-1)} N^{\alpha\beta\gamma}(x_1, x_2) + \frac{N}{(N^2-1)(N^2-4)} d^{abc} O^{\alpha\beta\gamma}(x_1, x_2), \quad (3.29)$$

It has the symmetry of SU(3) group when considering the hadron scatterings, thus Eq.(3.29) can be decomposed into symmetry part and anti-symmetry part as

$$M_{F,abc}^{\alpha\beta\gamma}(x_1, x_2) = -\frac{i}{24} f^{abc} N^{\alpha\beta\gamma}(x_1, x_2) + \frac{3}{40} d^{abc} O^{\alpha\beta\gamma}(x_1, x_2). \quad (3.30)$$

whereas $O^{\alpha\beta\gamma}(x_1, x_2), N^{\alpha\beta\gamma}(x_1, x_2)$ are given by [37]

$$\begin{aligned}
N^{\alpha\beta\gamma}(x_1, x_2) &= gi \int \tfrac{d\lambda}{2\pi} \tfrac{d\mu}{2\pi} e^{i\lambda x} e^{i\mu(x_2-x_1)} \langle pS_\perp | if^{bca} F_b^{\beta n}(0) F_c^{\gamma n}(\mu n) F_a^{\alpha n}(\lambda n) | pS_\perp \rangle, \\
O^{\alpha\beta\gamma}(x_1, x_2) &= gi \int \tfrac{d\lambda}{2\pi} \tfrac{d\mu}{2\pi} e^{i\lambda x} e^{i\mu(x_2-x_1)} \langle pS_\perp | d^{bca} F_b^{\beta n}(0) F_c^{\gamma n}(\mu n) F_a^{\alpha n}(\lambda n) | pS_\perp \rangle \quad (3.31)
\end{aligned}$$

From direct observation, one can discover that these functions have the symmetry of

$$\begin{aligned} O(x_1,x_2) &= O(x_2,x_1), O(-x_1,-x_2) = O(x_2,x_1) \\ N(x_1,x_2) &= N(x_2,x_1), N(-x_1,-x_2) = -N(x_2,x_1). \end{aligned} \tag{3.32}$$

We can perform the expansion for respective matrix elements up to twist-3 order as

$$\begin{aligned} & O^{\alpha\beta\gamma}(x_1,x_2) \\ =\ & 2iM[g_\perp^{\alpha\beta}\epsilon^{\gamma pnS_\perp}O(x_1,x_2) + g_\perp^{\beta\gamma}\epsilon^{\alpha pnS_\perp}O(x_2,x_2-x_1) + g_\perp^{\alpha\gamma}\epsilon^{\beta pnS_\perp}O(x_1,x_1-x_2)] + \cdots \\ & N^{\alpha\beta\gamma}(x_1,x_2) \\ =\ & 2iM[g_\perp^{\alpha\beta}\epsilon^{\gamma pnS_\perp}N(x_1,x_2) - g_\perp^{\beta\gamma}\epsilon^{\alpha pnS_\perp}N(x_2,x_2-x_1) - g_\perp^{\alpha\gamma}\epsilon^{\beta pnS_\perp}N(x_1,x_1-x_2)] + \cdots . \end{aligned} \tag{3.33}$$

It will be suppressed by $\frac{Q}{M}$. The expansions for $\Phi_\partial^{\alpha\beta\gamma}(x)$ is given by[32, 36, 37]

$$\begin{aligned} & \Phi_\partial^{\alpha\beta\gamma}(x) \\ =\ & \int \frac{d\lambda}{2\pi} e^{i\lambda x}\langle pS_\perp|F^{\beta n}(0)F^{\alpha n}(\lambda n)|pS_\perp\rangle(i\overleftarrow{\partial}_\perp^\gamma) \\ \equiv\ & \lim_{\xi_\perp\to 0}\int \frac{d\lambda}{2\pi} e^{i\lambda x}\langle pS_\perp|\Big(F^{\beta n}(0)[0,\infty n]\Big)_a \frac{d}{d\xi_{\perp\gamma}}\Big([\infty n+\xi_\perp,\lambda n+\xi_\perp]F^{\alpha n}(\lambda n+\xi_\perp)\Big)_a|pS_\perp\rangle \\ =\ & \frac{M_N}{2}g_\perp^{\alpha\beta}\epsilon^{pnS_\perp\gamma}G_T^{(1)}(x) + i\frac{M_N}{2}\epsilon^{pn\alpha\beta}S_\perp^\gamma\Delta G_T^{(1)}(x) + \frac{M_N}{8}\Big(\epsilon^{pnS_\perp\{\alpha}g_\perp^{\beta\}\gamma} \\ & +\epsilon^{pn\gamma\{\alpha}S_\perp^{\beta\}}\Big)\Delta H_T^{(1)}(x) + \cdots , \end{aligned} \tag{3.34}$$

where $\Delta G_T^{(1)}(x)$ is cancelled with an imaginary contribution and $G_T^{(1)}(x)\&\Delta H_T^{(1)}(x)$ are constrained by

$$G_T^{(1)}(x) = -4\pi(N(x,x)-N(x,0)), \Delta H_T^{(1)}(x) = 8\pi N(x,0). \tag{3.35}$$

3.5 Twist-3 polarized cross section for J/ψ production in SIDIS

The hadronic tensor within the NRQCD framework can be generalized as

$$W^{\text{twist}-3}_{\rho\sigma} = \left\langle O^{J/\psi}(^3S_1^{[1]})\right\rangle \Big[\omega^\mu_\alpha\omega^\nu_\beta\omega^\lambda_\gamma \int \frac{dx}{x^2}\Phi^{\alpha\beta\gamma}_\partial \frac{\partial}{\partial k^\lambda} S_{\mu\nu,\rho\sigma}|_{xp} - \frac{1}{2}\omega^\mu_\alpha\omega^\nu_\beta\omega^\lambda_\gamma \frac{1}{x_1 - i\epsilon}\frac{1}{x_2 + i\epsilon}\frac{1}{x_2 - x_1 - i\epsilon}\int dx_1 dx_2 M^{\alpha\beta\gamma}_{F,abc} S^{abc}_{\mu\nu\lambda,\rho\sigma}\Big]. \quad (3.36)$$

We consider the Feynman diagrams in polarized situation with a coherent gluon originating from the nucleon connected with LHS part as FIG 3.5. The coherent gluon will

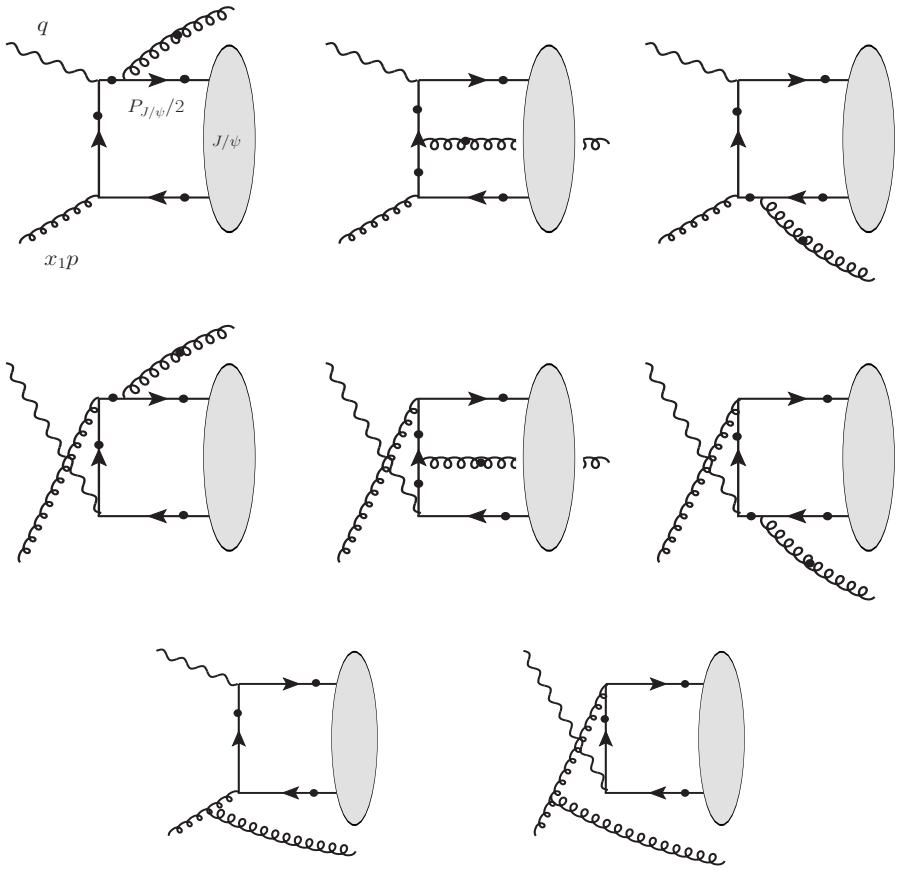

FIG 3.5 Diagrams that contribute to $H^{abc}_{L\mu\nu\lambda,\rho\sigma}(x_1 p, x_2 p)$. The external gluon line with the momentum $(x_2 - x_1)p$ is connected to one of the black dots. Thus there are 36 diagrams in this figure. We ignored some diagrams that obviously vanish.

introduce the freedom of transverse momentum that is significantly different from twist-2 case. In this paper we omit situations that the external gluon line connected the RHS for

convenience as it is the complex conjugate of the LHS. One can obtain the hard scattering part:

$$\begin{aligned} S_{\mu\nu,\rho\sigma} &= H_{\mu\nu\rho\sigma}(k)2\pi\delta(xp+q-P_{J/\psi})^2, \\ S^{abc}_{\mu\nu\lambda,\rho\sigma} &= H^{abc}_{L\mu\nu\lambda,\rho\sigma}\delta(x_2p+q-P_{J/\psi})^2 + H^{abc}_{R\mu\nu\lambda,\rho\sigma}\delta(x_1p+q-P_{J/\psi})^2. \end{aligned} \tag{3.37}$$

where $\delta(\cdots)$ denotes on-shell conditions for the radiation of gluon. We discover that $H^{abc}_{R\mu\nu\lambda,\rho\sigma}$ satisfies relation as follows through direct calculations.

$$H^{abc}_{R\mu\nu\lambda,\rho\sigma} = (H^{abc}_{L\mu\nu\lambda,\rho\sigma})^*. \tag{3.38}$$

We perform the conventional pole calculation as

$$\begin{aligned} & \frac{1}{x_1-i\epsilon}\frac{1}{x_2-x_1-i\epsilon}H^{abc}_{L\mu\nu\lambda,\rho\sigma}(x_1p,x_2p) \\ = & \frac{1}{x_1-i\epsilon}H^{1\,abc}_{L\mu\nu\lambda,\rho\sigma}(x_2p) + \frac{x_2}{(x_1-i\epsilon)^2}H^{2\,abc}_{L\mu\nu\lambda,\rho\sigma}(x_2p) \\ & + \frac{1}{x_2-x_1-i\epsilon}H^{3\,abc}_{L\mu\nu\lambda,\rho\sigma}(x_2p) + \frac{x_2}{(x_2-x_1-i\epsilon)^2}H^{4\,abc}_{L\mu\nu\lambda,\rho\sigma}(x_2p) \\ & + \frac{1}{x_1-Ax+i\epsilon}H^{5\,abc}_{L\mu\nu\lambda,\rho\sigma}(x_2p) + \frac{1}{x_1-(1-A)x-i\epsilon}H^{6\,abc}_{L\mu\nu\lambda,\rho\sigma}(x_2p), \\ & \frac{1}{x_2+i\epsilon}\frac{1}{x_2-x_1-i\epsilon}H^{abc}_{R\mu\nu\lambda,\rho\sigma}(x_1p,x_2p) \\ = & \frac{1}{x_2+i\epsilon}H^{1\,abc}_{R\mu\nu\lambda,\rho\sigma}(x_1p) + \frac{x_1}{(x_2+i\epsilon)^2}H^{2\,abc}_{R\mu\nu\lambda,\rho\sigma}(x_1p) \\ & + \frac{1}{x_2-x_1-i\epsilon}H^{3\,abc}_{R\mu\nu\lambda,\rho\sigma}(x_1p) + \frac{x_1}{(x_2-x_1-i\epsilon)^2}H^{4\,abc}_{R\mu\nu\lambda,\rho\sigma}(x_1p) \\ & + \frac{1}{x_2-Ax-i\epsilon}H^{5\,abc}_{R\mu\nu\lambda,\rho\sigma}(x_1p) + \frac{1}{x_2-(1-A)x+i\epsilon}H^{6\,abc}_{R\mu\nu\lambda,\rho\sigma}(x_1p), \end{aligned} \tag{3.39}$$

where

$$A = \frac{Q^2(1+\hat{x}-z_f)+m^2_{J/\psi}\hat{x}}{Q^2(2-z_f)}. \tag{3.40}$$

These $A-$ dependent terms are originating from internal propagators of the diagram and we shall decompose the amplitude to clarify the specific structure of pole. We can obtain

the expressions of hadronic tensor by taking the exchange of $x' \to x - x'$ as

$$
\begin{aligned}
& W^{\text{twist}-3}_{\rho\sigma}(p,q,P_{J/\psi}) \\
= \; & 2\pi\langle O^{J/\psi}(^3S_1^{[1]})\rangle \int \frac{dx}{x^2}\delta\Big((xp+q-P_{J/\psi})^2\Big) \\
& \Big\{\Big(x\frac{d}{dx}G_T^{(1)}(x) - 2G_T^{(1)}(x)\Big)H^{G1}_{\rho\sigma} + G_T^{(1)}(x)H^{G2}_{\rho\sigma} \\
& +\Big(x\frac{d}{dx}\Delta H_T^{(1)}(x) - 2\Delta H_T^{(1)}(x)\Big)H^{H1}_{\rho\sigma} + \Delta H_T^{(1)}(x)H^{H2}_{\rho\sigma} \\
& + \int dx' \sum_i \Big[\Big(\frac{1}{x-x'-i\epsilon}H^{Ni}_{1L\rho\sigma} + \frac{x}{(x-x'-i\epsilon)^2}H^{Ni}_{2L\rho\sigma} + \frac{1}{x'-Ax+i\epsilon}H^{Ni}_{3L\rho\sigma}\Big)N^i(x',x) \\
& +\Big(\frac{1}{x-x'+i\epsilon}H^{Ni}_{1R\rho\sigma} + \frac{x}{(x-x'+i\epsilon)^2}H^{Ni}_{2R\rho\sigma} + \frac{1}{x'-Ax-i\epsilon}H^{Ni}_{3R\rho\sigma}\Big)N^i(x,x') \\
& +\Big(\frac{1}{x-x'-i\epsilon}H^{Oi}_{1L\rho\sigma} + \frac{x}{(x-x'-i\epsilon)^2}H^{Oi}_{2L\rho\sigma} + \frac{1}{x'-Ax+i\epsilon}H^{Oi}_{3L\rho\sigma}\Big)O^i(x',x) \\
& +\Big(\frac{1}{x-x'+i\epsilon}H^{Oi}_{1R\rho\sigma} + \frac{x}{(x-x'+i\epsilon)^2}H^{Oi}_{2R\rho\sigma} + \frac{1}{x'-Ax-i\epsilon}H^{Oi}_{3R\rho\sigma}\Big)O^i(x,x')\Big]\Big\}, \quad (3.41)
\end{aligned}
$$

where we used the shorthand notations as follows for simplicity

$$
\begin{aligned}
N^{1,2,3}(x',x) &= \{N(x',x), N(x,x-x'), N(x',x'-x)\}, \\
O^{1,2,3}(x',x) &= \{O(x',x), O(x,x-x'), O(x',x'-x)\}. \quad (3.42)
\end{aligned}
$$

One can perform the contour integrals like

$$
\begin{aligned}
\frac{1}{x'-x-i\epsilon} - \frac{1}{x'-x+i\epsilon} &= 2\pi i\delta(x'-x), \\
\frac{1}{x'-Ax-i\epsilon} - \frac{1}{x'-Ax+i\epsilon} &= 2\pi i\delta(x'-Ax), \\
\frac{1}{(x'-x+i\epsilon)^2} - \frac{1}{(x'-x-i\epsilon)^2} &= 2\pi i\frac{\partial}{\partial x'}\delta(x'-x). \quad (3.43)
\end{aligned}
$$

These delta functions reflect the possible type of pole contribution. After submitting all the terms aforementioned and performing the integration, one can get the differential cross section formula for J/ψ production in color-singlet channel at twist-3 level shown as fol-

lows

$$\begin{aligned}
&\frac{d^6\Delta\sigma}{dx_B dQ^2 dz_f dP_T^2 d\phi d\chi} \\
&= \frac{\alpha_{em}^2\alpha_s^2 e_c^2(2\pi M_N)}{4\pi S_{ep}^2 x_B^2 Q^2}\Big(\mathcal{N}\langle O^{J/\psi}(^3S_1^{[1]})\rangle\Big)\sum_{i=1,\cdots,4,8,9}\mathcal{A}_i(\phi-\chi)\mathcal{S}_i(\Phi_S-\chi) \\
&\int\frac{dx}{x^2}\delta\Big[\frac{P_T^2}{Q^2}-\Big(1-\frac{1}{\hat{x}}+\frac{m_{J/\psi}^2}{z_f Q^2}\Big)\Big(1-\frac{1}{z_f}\Big)\Big]\Big[N(x,x)\sigma_i^{N1}+N(x,0)\sigma_i^{N2} \\
&+N(x,Ax)\sigma_i^{N3}+N(x,(1-A)x)\sigma_i^{N4}+N(Ax,-(1-A)x)\sigma_i^{N5}\Big], \qquad (3.44)
\end{aligned}$$

One can find that contributions from the C-odd function $O^i(x,x')$ are completely canceled. This implies a fact that the charm-anticharm pair is charge neutral or likewise C-even. Variable $\mathcal{S}$ stands for

$$\mathcal{S}_i(\Phi_S-\chi)=\sin(\Phi_S-\chi)(i=1,2,3,4),\ \cos(\Phi_S-\chi)(i=8,9) \qquad (3.45)$$

All of the hard cross sections are listed in Appendix. It turn out that the derivative terms $\frac{d}{dx}N(x,x)$ and $\frac{d}{dx}N(x,0)$ given by Eq.(3.43) will vanish in color-singlet model. The hard cross sections Eq.(A.6)-Eq.(A.11) imply that the most singular term with respect to small p_T is $p_T/(1-z_f)$ in color-singlet channel. It is negligible in low-p_T regions whereas enhanced in high-p_T region. Besides, we will observe that LDMEs are directly cancelled at the level of SSA next chapter.

Chapter 4 Numerical Simulations and Summary

In this chapter we perform numerical simulations for SSA in color-singlet J/ψ productions and end with a summary that provides predictions for future EIC experiment.

4.1 Numerical Simulations for the SSA in the J/ψ Production

The polarized cross section Eq.(3.44) can be expanded in terms of five structure functions $\mathcal{F}_i$ $(i = 1, 2, \cdots 5)$ as

$$\begin{aligned}\frac{d^6\Delta\sigma}{dx_B dQ^2 dz_f dP_T^2 d\phi d\chi} &= \sin(\phi_h - \phi_S)(\mathcal{F}_1 + \mathcal{F}_2\cos\phi_h + \mathcal{F}_3\cos 2\phi_h) \\ &\quad + \cos(\phi_h - \phi_S)(\mathcal{F}_4\sin\phi_h + \mathcal{F}_5\sin 2\phi_h),\end{aligned} \tag{4.1}$$

where the azimuthal dependences are given by

$$\phi_h = \phi - \chi, \quad \phi_h - \phi_S = \Phi_S - \chi. \tag{4.2}$$

The unpolarized cross section is defined as

$$\frac{d^6\sigma}{dx_B dQ^2 dz_f dP_T^2 d\phi d\chi} = \sigma_1^{\mathrm{U}} + \sigma_2^{\mathrm{U}}\cos\phi_h + \sigma_3^{\mathrm{U}}\cos 2\phi_h. \tag{4.3}$$

Here we perform simulations for the five normalized structure functions that can be constructed as [37]

$$\frac{\mathcal{F}_1}{\sigma_1^{\mathrm{U}}}, \quad \frac{\mathcal{F}_2}{2\sigma_1^{\mathrm{U}}}, \quad \frac{\mathcal{F}_3}{2\sigma_1^{\mathrm{U}}}, \quad \frac{\mathcal{F}_4}{2\sigma_1^{\mathrm{U}}}, \quad \frac{\mathcal{F}_5}{2\sigma_1^{\mathrm{U}}}. \tag{4.4}$$

The explicit form of $\mathcal{F}_1/\sigma_1^{\mathrm{U}}$ can be derived in terms of the variables defined in this thesis as

$$\begin{aligned}&\frac{\mathcal{F}_1}{\sigma_1^{\mathrm{U}}} \\ &= \frac{2\pi M_N}{[\frac{4}{y^2}(1 - y + \frac{y^2}{2})\hat{\sigma}_1 - 2\hat{\sigma}_2]\bar{x}G(\bar{x})}\Big[\frac{4}{y^2}(1 - y + \frac{y^2}{2})\Big(\sum_{i=1}^{5} N^i(\bar{x})\sigma_1^{Ni}\Big) - 2\Big(\sum_{i=1}^{5} N^i(\bar{x})\sigma_2^{Ni}\Big)\Big],\end{aligned} \tag{4.5}$$

where we have defined

$$\bar{x} = x_B\Big(1 + \frac{m_{J/\psi}^2}{z_f Q^2} + \frac{P_T^2}{Q^2}\frac{z_f}{1-z_f}\Big). \tag{4.6}$$

$$N^{1,2,3,4,5}(x) = \{N(x,x),\ N(x,0),\ N(x,Ax),\ N(x,(1-A)x),\ N(Ax,-(1-A)x)\}, \tag{4.7}$$

Other normalized structure functions can be obtained following the same procedure. From calculation one can observe that the LDMEs are directly cancelled as stated. We perform the numerical calculations based on models in [38]

$$\begin{aligned} &\text{model 1}: N(x,0) = N(x,x) = 0.002xG(x), \\ &\text{model 2}: N(x,0) = N(x,x) = 0.0005\sqrt{x}G(x). \end{aligned} \tag{4.8}$$

It has been proved that magnitudes of these models represent upper bound of the experimental data[39] where each structure function shall rely on these five types of C-even functions as $N(x,x)$, $N(x,0)$, $N(x,Ax)$, $N(x,(1-A)x)\&N(Ax,-(1-A)x)$. Thus one can separately obtain contributions with respect to these normalized functions within two models before. In spite of the limited knowledge in $N(x,Ax)$, $N(x,(1-A)x)\&N(Ax,-(1-A)x)$, we perform the same approximation for these A-dependent functions. In this paper we assume the kinematic variables fixed in EIC regime [26] as follows.

$$\sqrt{S_{ep}} = 45\text{GeV},\ \ Q^2 = 10\text{GeV}^2,\ \ x_B = 0.005,\ \ P_{J/\psi}^{\perp} = 2\text{GeV}. \tag{4.9}$$

4.2 Analysis and Summary

Results of numerical simulations are shown as follows in terms of model 1 and model 2. We have found that each normalized structure functions reflect different qualitative behaviours. These simulations are crucial in clarifying the specific function which

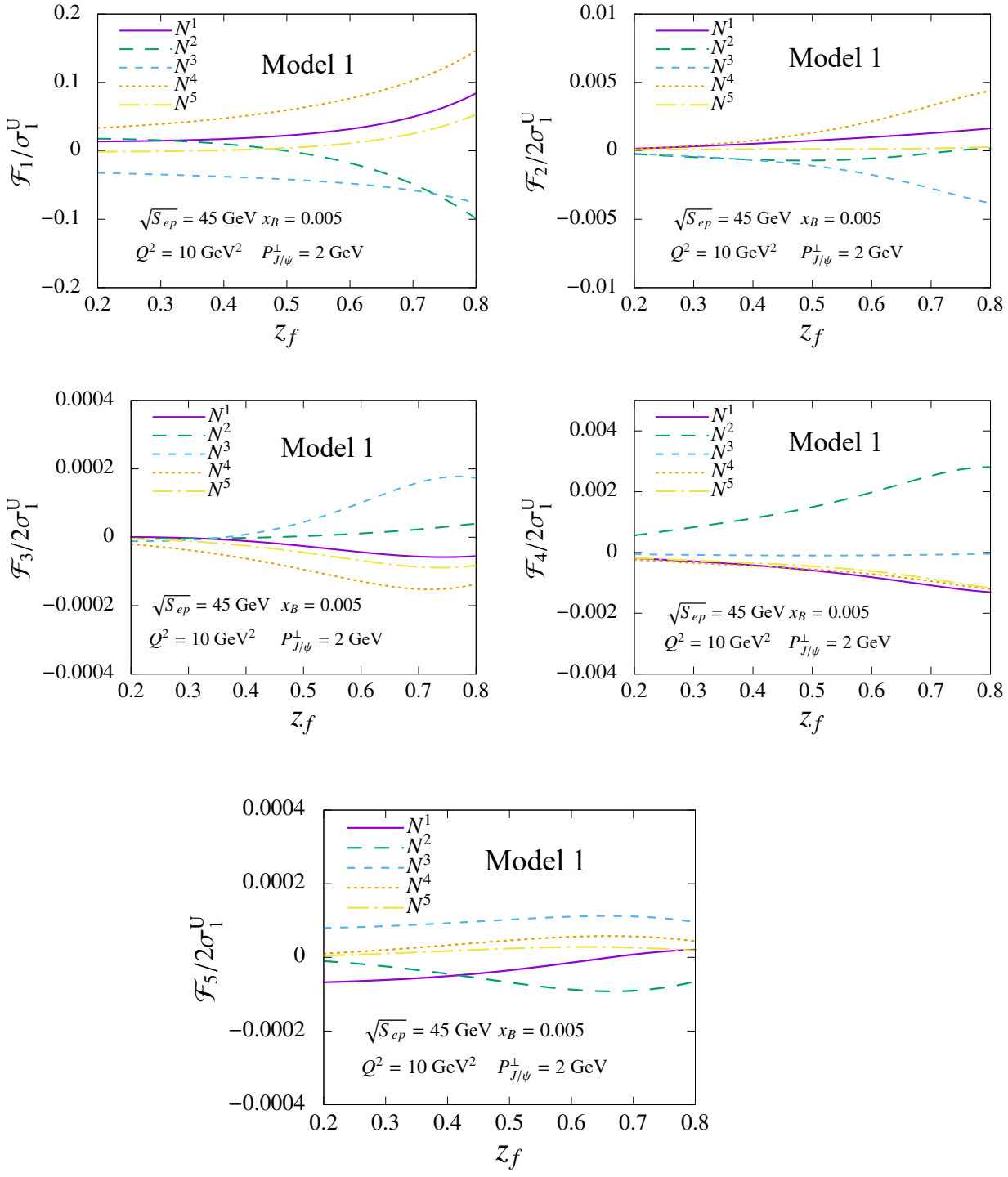

FIG 4.1 Numerical calculations for the normalized structure functions in (4.4). $N^{1,2,3,4,5}$ respectively show the contribution from the five functions $N(x,x)$, $N(x,0)$, $N(x,Ax)$, $N(x,(1-A)x)$, $N(Ax,-(1-A)x)$ with the model 1 function (4.8).

is dominant in J/ψ SSA through comparing with the data from EIC. We perform qualitative analysis to the behaviour of each C-even functions in normalized structure function in

different figures. Throughout the simulation, it reads that the $\mathcal{F}_1/\sigma_1^{\mathrm{U}}$ shall be the possible source of large SSA. In the first picture of FIG 4.1, contribution of the $N(x,x)$ to SSA remains constant in small z_f, then starts to increase slowly and could give a max asymmetry of around tens percent in large z_f. And for $N(x,0)$, it is followed by the $N(x,x)$, then decreases directly which could give the contribution of minus tens percent of the SSA. Simulations aforementioned have implied that $N(x,x)\&N(x,0)$ are sensitive to z_f and give a significant contribution to SSA in large z_f. Thus $\mathcal{F}_1/\sigma_1^{\mathrm{U}}$ could be the ideal observable for the investigation of large asymmetry. In addition, the $N(x,Ax)$ keeps almost constant throughout the simulation with only few drops in large z_f. It could give the asymmetry of near -7% that cannot be ignored. The $N(x,(1-A)x)$ shall be the most notable function as it keeps increasing in the full picture and have a contribution of near fifteens percent of the SSA. Besides, the $N(Ax,-(1-A)x)$ doesn't have any contributions till large z_f and could give the contribution of near 5% to the SSA. Consequently, we can state that the behaviours of $N(x,x)$, $N(x,0)$, $N(x,(1-A)x)$ and $N(Ax,-(1-A)x)$ in large z_f have shown that the $\mathcal{F}_1/\sigma_1^{\mathrm{U}}$ is ideal observable for the investigation of large SSA. Compared with the first normalized structure function, the contribution of $\frac{\mathcal{F}_2}{2\sigma_1^{\mathrm{U}}}$ to the SSA are not so significant for all C-even functions and most of them are not sensitive to z_f. One can find that the $N(x,(1-A)x)\&N(x,Ax)$ are the only function sensitive to z_f while $N(x,x)$, $N(x,0)\&N(x,Ax)$ doesn't make noticeable contribution throughout the simulation. Their predicted contribution to the SSA is around 0.5% and thus the $\frac{\mathcal{F}_2}{2\sigma_1^{\mathrm{U}}}$ could not explain the large SSA.

The situation is also similar for the $\mathcal{F}_3/\sigma_1^{\mathrm{U}}$. As for the simulation of $\mathcal{F}_3/\sigma_1^{\mathrm{U}}$, one can find that all of the five C-even functions have their own dependence with respect to z_f. The $N(x,Ax)\&N(x,(1-A)x)$ have the most singularities and other C-even functions don't give a significant contribution. Among them, it is the $N(x,Ax)$ that contributes the most but can still not be origin of the observed large SSA. It gives around 0.02% of the asymmetry while SSA was once stated to be over tens percent. Within the simulation for the $\mathcal{F}_4/\sigma_1^{\mathrm{U}}$, we discover that almost all of the contribution from five C-even functions to

the SSA have significant changes except for the $N(x, Ax)$ that almost doesn't have any contributions.

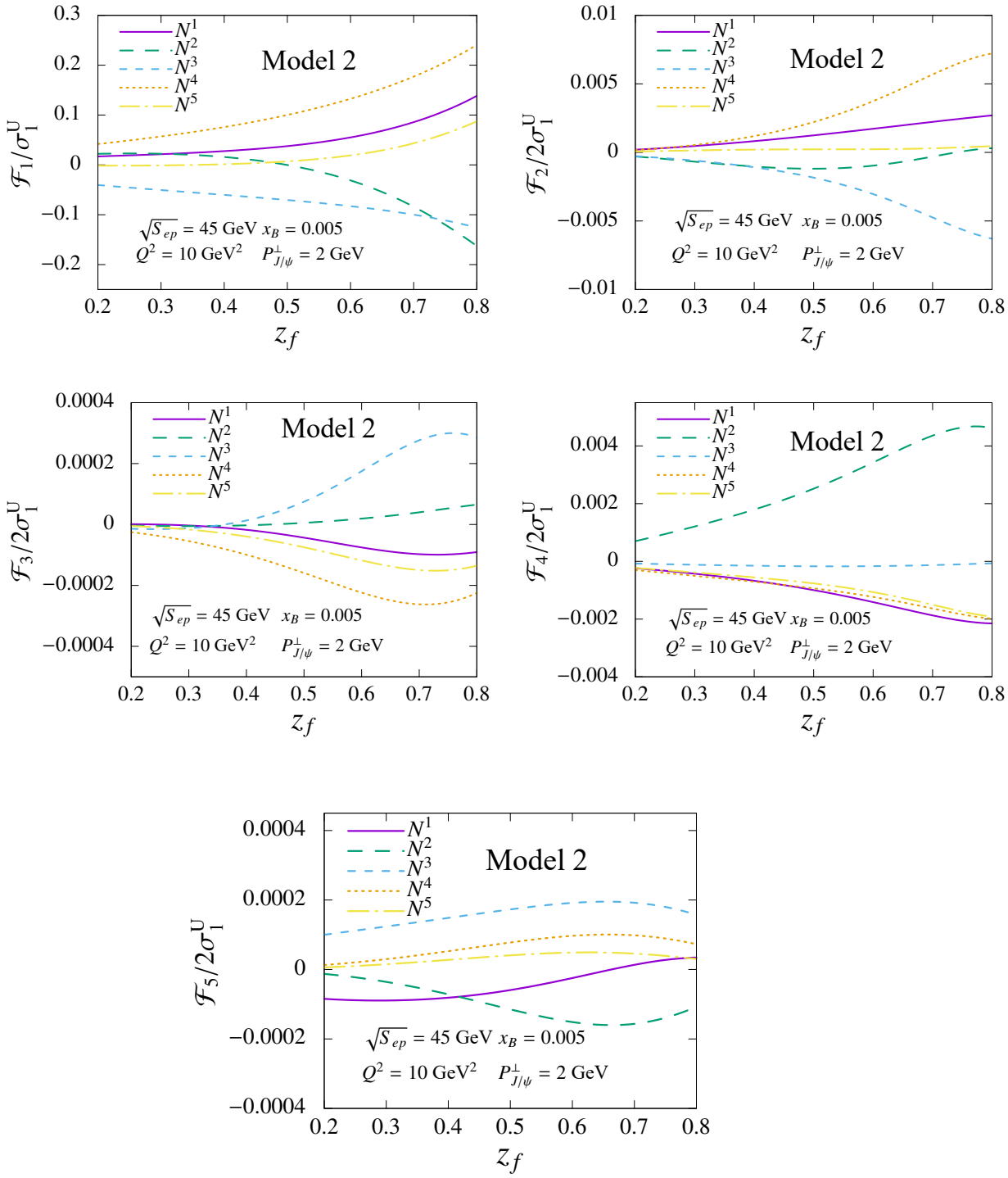

FIG 4.2 Numerical calculations for the normalized structure functions with the model 2 function (4.8).

Besides, behaviours of $N(x,(1-A)x)\&N(Ax,-(1-A)x)$ are uniformly similar and decrease in the simulation. As for $N(x,0)$, it keeps increasing with respect to z_f and has the major contribution for the SSA of $\mathcal{F}_4/\sigma_1^{\mathrm{U}}$. However, the $\mathcal{F}_4/\sigma_1^{\mathrm{U}}$ can not be the possible source of large SSA as the simulation shows it has contributed about 0.3% of the asymmetry. This also occurs in $\mathcal{F}_5/\sigma_1^{\mathrm{U}}$ where all of the five C-even functions are not sensitive to z_f. The predicted SSA is relatively less than 0.2%.

In model 1, one can attribute the possible source of the large SSA to the $\mathcal{F}_1/\sigma_1^{\mathrm{U}}$ from simulations and analysis before. Behaviours of these five C-even functions are sensitive in large z_f regions and therefore, the $\mathcal{F}_1/\sigma_1^{\mathrm{U}}$ could be the supposed observable in future experiments. Besides, simulations imply that behaviours of these C-even functions are not sensitive in small z_f. It can be evaluated in the level of hard cross sections. One may find the most singular term in hard cross section is proportional to $\frac{q_T}{1-z_f}$ which is constant in small z_f and divergent in large z_f. However, different behaviours with respect to the normalized structure functions haven't been fully understood and ask for deeper understanding of the gluon Sivers function. Theoretical studies on these normalized structure functions are crucial for the study of the observed large asymmetry.

Similar analysis is carried on the second model and find that there doesn't exist a significant difference about the qualitative behaviour between two models during the simulations. The contribution from these five types of functions shows different qualitative behaviours in each normalized structure function. These simulations are crucial for the investigation of gluon Sivers effect and provide theoretical predictions for future experiments. Our simulations show that the difference in the x-dependence between the model 1 and 2 does not cause a significant change in the qualitative behaviours. However, it turns out that the magnitudes of the contribution are uniformly increased in the model 2 compared to the model 1. This reflects the fact that the model 2 is more singular with respect to x and, therefore, it is enhanced at the small value of x_B. The observation of the enhancement could give us the information about the small-x behaviour of the C-even function. The future EIC experiment plans to investigate the proton structure in a wide range of

x_B, $10^{-3} \lesssim x_B \lesssim 0.5$. The measurement of J/ψ SSA at the EIC is a great opportunity to understand the small-x behaviour of the higher twist gluon distribution function.

We have carried out the first analytical calculation for the twist-3 gluon Sivers contribution to SSA in J/ψ production at color-singlet channel. We have found that the heavy quarkonium productions are ideal observables for investigations of C-even type twist-3 gluon Sivers functions. Because other sources of the nonperturbative effect, C-odd type twist-3 gluon contribution and the hadronization effect from J/ψ(LDME), are canceled at the level of the SSA. From direct calculations, we have found that cancellations also occur in derivative terms as $\frac{d}{dx}N(x,x)$ and $\frac{d}{dx}N(x,0)$ whereas non-derivative terms $N(x,x)$ and $N(x,0)$ survive. It was once stated that the SSA should vanish in ep collisions at color-singlet channel in heavy quarkonium productions[40]. Our result shows that this statement does not hold in high $P_{J/\psi}^{\perp}$ region. Besides, we have performed numerical simulations for the five normalized structure functions within two different models at EIC regime. We find out that the normalized function $\frac{\mathcal{F}_1}{2\sigma_1^{\mathrm{U}}}$ could give the large asymmetry. It provides a new way to investigate the gluon Sivers effect. The future EIC experiment is expected to provide rich data about little-known Sivers function and theoretical predictions made by our work is crucial for the EIC .

Bibliography

[1] E. Rutherford. LIV. Collision of α Particles with Light Atoms. IV. An Anomalous Effect in Nitrogen [J]. Phil. Mag. Ser. 6. 1919, 37 (222): 581–587.

[2] Chadwick J. Possible Existence of a Neutron [J]. Nature. 1932, 129: 312.

[3] Griffiths D J. Introduction to Elementary Particles [M]. 1987.

[4] Gell-Mann M. A Schematic Model of Baryons and Mesons [J]. Phys. Lett. 1964, 8: 214–215.

[5] Zweig G. An SU(3) Model for Strong Interaction Symmetry and Its Breaking. Version 1 [J]. 1964.

[6] Bjorken J D, Paschos E A. Inelastic Electron Proton and Gamma Proton Scattering, and the Structure of the Nucleon [J]. Phys. Rev. 1969, 185: 1975–1982.

[7] Feynman R P. The Behavior of Hadron Collisions at Extreme Energies [J]. Conf. Proc. C. 1969, 690905: 237–258.

[8] Gross D J, Wilczek F. Ultraviolet Behavior of Nonabelian Gauge Theories [J]. Phys. Rev. Lett. 1973, 30: 1343–1346.

[9] Callan C G, Jr, Gross D J. High-energy ElectroProduction and the Constitution of the Electric Current [J]. Phys. Rev. Lett. 1969, 22: 156–159.

[10] Bosetti P C, et al. Analysis of Nucleon Structure Functions in CERN Bubble Chamber Neutrino Experiments [J]. Nucl. Phys. B. 1978, 142: 1–28.

[11] Aid S, et al. A Measurement and QCD Analysis of the Proton Structure Function $f_2(x, q^2)$ at HERA [J]. Nucl. Phys. B. 1996, 470: 3–40.

[12] Altarelli G, Parisi G. Asymptotic Freedom in Parton Language [J]. Nucl. Phys. B. 1977, 126: 298–318.

[13] Kane G L, Pumplin J, Repko W. Transverse Quark Polarization in Large p_T Reactions, e^+e^- Jets, and Lepton Production: A Test of QCD [J]. Phys. Rev. Lett. 1978, 41: 1689.

[14] Abdulhamid M, et al. Longitudinal and Transverse Spin Transfer to Λ and $\bar{\Lambda}$ Hyperons in Polarized $p+p$ Collisions at $\sqrt{s} = 200$ GeV [J]. Phys. Rev. D. 2024, 109 (1): 012004.

[15] Lin T. Exploring the Spin Structure of the Nucleon at STAR [C]. In 30th International Conference on Ultrarelativstic Nucleus-Nucleus Collisions. 2 2024.

[16] Liang X. Transverse Single-Spin Asymmetry for Inclusive and Diffractive Electromagnetic Jets at Forward Rapidity in $p^{\uparrow} + p$ Collisions at $\sqrt{s} = 200$ GeV and 510 GeV at STAR [J]. 2023.

[17] Sivers D W. Single Spin Production Asymmetries from the Hard Scattering of Point-Like Constituents [J]. Phys. Rev. D. 1990, 41: 83.

[18] Anselmino M, Boglione M, D'Alesio U, et al. The Role of Cahn and Sivers Effects in Deep Inelastic Scattering [J]. Phys. Rev. D. 2005, 71: 074006.

[19] Airapetian A, et al. Single-spin Asymmetries in Semi-Inclusive Deep-Inelastic Scattering on A Transversely Polarized Hydrogen Target [J]. Phys. Rev. Lett. 2005, 94: 012002.

[20] Alekseev M, et al. Collins and Sivers Asymmetries for Pions and Kaons in Muon-Deuteron DIS [J]. Phys. Lett. B. 2009, 673: 127–135.

[21] Ageev E S, et al. A New Measurement of the Collins and Sivers Asymmetries on A Transversely Polarised Deuteron Target [J]. Nucl. Phys. B. 2007, 765: 31–70.

[22] Qiu J-w, Sterman G F. Single Transverse Spin Asymmetries in Hadronic Pion Production [J]. Phys. Rev. D. 1999, 59: 014004.

[23] Kanazawa K, Koike Y, Metz A, et al. Operator Constraints for Twist-3 Functions and Lorentz Invariance Properties of Twist-3 Observables [J]. Phys. Rev. D. 2016, 93 (5): 054024.

[24] Kanazawa K, Koike Y. A Phenomenological Study on Single Transverse-Spin Asymmetry for Inclusive Light-Hadron Productions at RHIC [J]. Phys. Rev. D. 2011, 83: 114024.

[25] Gamberg L, Malda M, Miller J A, et al. Updated QCD Global Analysis of Single Transverse-Spin Asymmetries: Extracting H~, and the Role of the Soffer Bound and Lattice QCD [J]. Phys. Rev. D. 2022, 106 (3): 034014.

[26] Accardi A, et al. Electron Ion Collider: The Next QCD Frontier: Understanding the Glue That Binds Us All [J]. Eur. Phys. J. A. 2016, 52 (9): 268.

[27] Anderle D P, et al. Electron-Ion Collider in China [J]. Front. Phys. (Beijing). 2021, 16 (6): 64701.

[28] Ellis R K, Furmanski W, Petronzio R. Unraveling Higher Twists [J]. Nucl. Phys. B. 1983, 212: 29.

[29] Peskin M E, Schroeder D V. An Introduction to Quantum Field Theory [M]. Reading, USA: Addison-Wesley, 1995.

[30] Jaffe R L. Spin, Twist and Hadron Structure in Deep Inelastic Processes [C]. In Ettore Majorana International School of Nucleon Structure: 1st Course: The Spin Structure of the Nucleon. 1 1996: 42–129.

[31] Meng R-b, Olness F I, Soper D E. Semiinclusive Deeply Inelastic Scattering at Electron - Proton Colliders [J]. Nucl. Phys. B. 1992, 371: 79–110.

[32] Yoshida S, Zheng D. Reformulation of the Twist-3 Gluon Sivers Effect toward An Application to Heavy Quarkonium Production [J]. Phys. Rev. D. 2022, 106 (3): 034019.

[33] Brambilla N, et al. Heavy Quarkonium: Progress, Puzzles, and Opportunities [J]. Eur. Phys. J. C. 2011, 71: 1534.

[34] Brambilla N, et al. Heavy Quarkonium Physics [J]. 2004.

[35] Bodwin G T, Braaten E, Lepage G P. Rigorous QCD Analysis of Inclusive Annihilation and Production of Heavy Quarkonium [J]. Phys. Rev. D. 1995, 51: 1125–1171. [Erratum: Phys.Rev.D 55, 5853 (1997)].

[36] Chen L, Xing H, Yoshida S. The Twist-3 Gluon Contribution to Sivers Asymmetry in J/ψ Production in Semi-Inclusive Deep Inelastic Scattering [J]. Phys. Rev. D. 2023, 108 (5): 054021.

[37] Beppu H, Koike Y, Tanaka K, et al. Contribution of Twist-3 Multi-Gluon Correlation Functions to Single Spin Asymmetry in Semi-Inclusive Deep Inelastic Scattering [J]. Phys. Rev. D. 2010, 82: 054005.

[38] Koike Y, Yoshida S. Probing the Three-Gluon Correlation Functions by the Single Spin Asymmetry in $p^{\uparrow}p \to DX$ [J]. Phys. Rev. D. 2011, 84: 014026.

[39] Abdulameer N J, et al. Improving Constraints on Gluon Spin-Momentum Correlations in Transversely Polarized Protons via Midrapidity Open-Heavy-Flavor Electrons in $p^{\uparrow} + p$ Collisions at $\sqrt{s} = 200$ GeV [J]. Phys. Rev. D. 2023, 107 (5): 052012.

[40] Yuan F. Heavy Quarkonium Production in Single Transverse Polarized High Energy Scattering [J]. Phys. Rev. D. 2008, 78: 014024.

Appendix A Hard cross sections

(1) Hard cross sections of the unpolarized cross section in (3.4)

$$\begin{aligned}\hat{\sigma}_1 &= \frac{1}{z_f^2[Q^2(-1+\hat{x})+m_{J/\psi}^2\hat{x}]^2[m_{J/\psi}^2\hat{x}+Q^2(1+\hat{x}-z_f)]^2}64m_{J/\psi}^2\\ &\hat{x}^2\Big(m_{J/\psi}^6\hat{x}^2(1-z_f+z_f^2)+m_{J/\psi}^2Q^4[1+(-2+4\hat{x}-7\hat{x}^2)z_f+(3-18\hat{x}+22\hat{x}^2)z_f^2\\ &-2(1-8\hat{x}+9\hat{x}^2)z_f^3+(1-6\hat{x}+6\hat{x}^2)z_f^4]+Q^6(-1+\hat{x})z_f[-z_f+\hat{x}(-1+2z_f)]\\ &+m_{J/\psi}^4Q^2\hat{x}[z_f(-3+3z_f-2z_f^2)+\hat{x}(-5+17z_f-15z_f^2+6z_f^3)]\Big) \qquad (A.1)\end{aligned}$$

$$\begin{aligned}\hat{\sigma}_2 &= \frac{1}{z_f^2[Q^2(-1+\hat{x})+m_{J/\psi}^2\hat{x}]^2[m_{J/\psi}^2\hat{x}+Q^2(1+\hat{x}-z_f)]^2}\\ &\times64m_{J/\psi}^2Q^2\hat{x}^2\Big(Q^4(-1+\hat{x})^2z_f^2+2m_{J/\psi}^2Q^2(-1+\hat{x})\hat{x}z_f(-1+6z_f-6z_f^2+2z_f^3)\\ &+m_{J/\psi}^4\hat{x}^2(-2+10z_f-11z_f^2+4z_f^3)\Big) \qquad (A.2)\end{aligned}$$

$$\begin{aligned}\hat{\sigma}_3 &= \frac{1}{z_f[Q^2(-1+\hat{x})+m_{J/\psi}^2\hat{x}]^2[m_{J/\psi}^2\hat{x}+Q^2(1+\hat{x}-z_f)]^2}\\ &\times64m_{J/\psi}^2QP_T\hat{x}^3\Big(Q^4(-1+\hat{x})z_f+m_{J/\psi}^4\hat{x}(3-4z_f+2z_f^2)+m_{J/\psi}^2Q^2[z_f(-3\\ &+4z_f-2z_f^2)+\hat{x}(-1+9z_f-10z_f^2+4z_f^3)]\Big) \qquad (A.3)\end{aligned}$$

$$\begin{aligned}\hat{\sigma}_4 &= -\frac{1}{z_f^2[Q^2(-1+\hat{x})+m_{J/\psi}^2\hat{x}]^2[m_{J/\psi}^2\hat{x}+Q^2(1+\hat{x}-z_f)]^2}(64m_{J/\psi}^4\hat{x}^3\\ &(-1+z_f)[m_{J/\psi}^2\hat{x}+Q^2(-1+\hat{x})z_f][m_{J/\psi}^2+Q^2(-1+4z_f-2z_f^2)]) \qquad (A.4)\end{aligned}$$

$$\hat{\sigma}_8 = \hat{\sigma}_9 = 0 \qquad (A.5)$$

(2) Hard cross sections of $N(x,x)$ in (3.44)

$$
\begin{aligned}
\hat{\sigma}_1^{N1} = & \frac{-1}{(1-z_f)z_f^2 Q^2[Q^2(-1+\hat{x})+m_{J/\psi}^2\hat{x}]^3[m_{J/\psi}^2\hat{x}+Q^2(1+\hat{x}-z_f)]^3} \\
& \times 128 m_{J/\psi}^2 P_T \hat{x}^3\Big(2m_{J/\psi}^{10}\hat{x}^4(5-6z_f+3z_f^2)+4Q^{10}(-1+\hat{x})z_f[1 \\
& -5z_f+3z_f^2-z_f^3+\hat{x}^3(-1+2z_f)+\hat{x}^2(z_f-4z_f^2)+\hat{x}(-2+7z_f-3z_f^2+2z_f^3)] \\
& +2m_{J/\psi}^8 Q^2\hat{x}^3[-2z_f(8-9z_f+5z_f^2)+\hat{x}(-9+58z_f-65z_f^2+26z_f^3)] \\
& +m_{J/\psi}^6 Q^4\hat{x}^2[18-34z_f+77z_f^2-63z_f^3+30z_f^4-16\hat{x}z_f(-3+19z_f \\
& -20z_f^2+8z_f^3)+2\hat{x}^2(-33+112z_f-65z_f^2-18z_f^3+24z_f^4)]+m_{J/\psi}^4 Q^6\hat{x}[z_f(\\
& -54+106z_f-123z_f^2+71z_f^3-24z_f^4)-4\hat{x}^2 z_f(-25+84z_f-27z_f^2-32z_f^3+24z_f^4)+ \\
& 2\hat{x}^3(-19+24z_f+81z_f^2-114z_f^3+48z_f^4)+2\hat{x}(-9+65z_f-123z_f^2+224z_f^3 \\
& -177z_f^4+62z_f^5)]+m_{J/\psi}^2 Q^8[4-12z_f+47z_f^2-74z_f^3+67z_f^4-32z_f^5+8z_f^6 \\
& +4\hat{x}^4 z_f(-13+41z_f-35z_f^2+12z_f^3)-8\hat{x}^3 z_f(-3+31z_f^2-32z_f^3+12z_f^4)+\hat{x}z_f(28 \\
& -220z_f+363z_f^2-359z_f^3+188z_f^4-48z_f^5)+\hat{x}^2(12-84z_f+229z_f^2-157z_f^3+152z_f^4 \\
& -116z_f^5+48z_f^6)]\Big)
\end{aligned}
\tag{A.6}
$$

$$
\begin{aligned}
\hat{\sigma}_2^{N1} = & \frac{-1}{(1-z_f)z_f^2[Q^2(-1+\hat{x})+m_{J/\psi}^2\hat{x}]^3[m_{J/\psi}^2\hat{x}+Q^2(1+\hat{x}-z_f)]^3} \\
& \times 512 m_{J/\psi}^2 P_T \hat{x}^3\Big(Q^8(-1+\hat{x})^2 z_f^2(3+\hat{x}^2-2z_f-2\hat{x}z_f+z_f^2)+m_{J/\psi}^8\hat{x}^4(-4 \\
& +20z_f-23z_f^2+8z_f^3)+2m_{J/\psi}^6 Q^2\hat{x}^3[z_f(5-26z_f+29z_f^2-10z_f^3)+2\hat{x}(-2+9z_f-6z_f^2 \\
& -2z_f^3+2z_f^4)]+m_{J/\psi}^4 Q^4\hat{x}^2[-4+24z_f-50z_f^2+84z_f^3-67z_f^4+20z_f^5+2\hat{x}z_f(6-29z_f \\
& +13z_f^2+12z_f^3-8z_f^4)+2\hat{x}^2(-2+6z_f+11z_f^2-20z_f^3+8z_f^4)]+2m_{J/\psi}^2 Q^6\hat{x}z_f[3-21z_f \\
& +36z_f^2-35z_f^3+18z_f^4-4z_f^5+2\hat{x}^3(-1+6z_f-6z_f^2+2z_f^3)+\hat{x}^2(1-4z_f-17z_f^2+22z_f^3 \\
& -8z_f^4)+\hat{x}(-2+13z_f-7z_f^2+9z_f^3-10z_f^4+4z_f^5)]\Big)
\end{aligned}
\tag{A.7}
$$

$$\hat{\sigma}_3^{N1} = \frac{1}{z_f^3 Q[Q^2(-1+\hat{x})+m_{J/\psi}^2\hat{x}]^3[m_{J/\psi}^2\hat{x}+Q^2(1+\hat{x}-z_f)]^3}$$
$$\times 128 m_{J/\psi}^2\hat{x}^2\Big(2m_{J/\psi}^{10}\hat{x}^5(13-21z_f+10z_f^2)+Q^{10}(-1+\hat{x})^2z_f^2[4\hat{x}^3+3(-1+z_f)$$
$$-8\hat{x}^2z_f+\hat{x}(9-8z_f+4z_f^2)]+m_{J/\psi}^8Q^2\hat{x}^4[z_f(-83+129z_f-62z_f^2)+\hat{x}(46$$
$$-78z_f^2+52z_f^3)]+m_{J/\psi}^6Q^4\hat{x}^3[22-48z_f+148z_f^2-177z_f^3+80z_f^4-\hat{x}z_f(101$$
$$+53z_f-226z_f^2+136z_f^3)+2\hat{x}^2(7+62z_f-79z_f^2+14z_f^3+16z_f^4)]$$
$$+m_{J/\psi}^2Q^8\hat{x}z_f[4+35z_f-92z_f^2+100z_f^3-58z_f^4+16z_f^5+\hat{x}^4(-2+66z_f-76z_f^2$$
$$+32z_f^3)+\hat{x}^3(1-71z_f-50z_f^2+120z_f^3-64z_f^4)+\hat{x}^2(-2+94z_f-15z_f^2-6z_f^3$$
$$-28z_f^4+32z_f^5)-\hat{x}(1+124z_f-233z_f^2+246z_f^3-150z_f^4+48z_f^5)]+m_{J/\psi}^4Q^6\hat{x}^2[z_f($$
$$-63+143z_f-192z_f^2+148z_f^3-54z_f^4)+2\hat{x}^3(-3+40z_f+z_f^2-50z_f^3+32z_f^4)$$
$$-\hat{x}^2z_f(17+245z_f-246z_f^2+16z_f^3+64z_f^4)+\hat{x}(-10+110z_f-123z_f^2$$
$$+248z_f^3-282z_f^4+132z_f^5)]\Big) \qquad \text{(A.8)}$$

$$\hat{\sigma}_4^{N1} = \frac{1}{z_f^2Q^2[Q^2(-1+\hat{x})+m_{J/\psi}^2\hat{x}]^3[m_{J/\psi}^2\hat{x}+Q^2(1+\hat{x}-z_f)]^3}$$
$$\times 128 m_{J/\psi}^4P_T\hat{x}^3\Big(2m_{J/\psi}^8\hat{x}^4(-5+3z_f)+2m_{J/\psi}^6Q^2\hat{x}^3[-6(-2+z_f)z_f+\hat{x}(-7$$
$$-11z_f+10z_f^2)]+m_{J/\psi}^4Q^4\hat{x}^2[-6-13z_f^2+6z_f^3+12\hat{x}z_f(1+6z_f-4z_f^2)+2\hat{x}^2(1$$
$$-27z_f+6z_f^2+8z_f^3)]+Q^8(-1+\hat{x})z_f[-3(-1+z_f)z_f+4\hat{x}^3(2-7z_f+4z_f^2)$$
$$-4\hat{x}^2(-1+7z_f-16z_f^2+8z_f^3)+\hat{x}(12-57z_f+76z_f^2-52z_f^3+16z_f^4)]$$
$$+m_{J/\psi}^2Q^6\hat{x}[-z_f(-104z_f+z_f^2)-4\hat{x}^2z_f(4-21z_f+8z_f^3)+2\hat{x}^3(3-9z_f-18z_f^2+$$
$$16z_f^3)+2\hat{x}(5-28z_f+35z_f^2-47z_f^3+22z_f^4)]\Big) \qquad \text{(A.9)}$$

$$\hat{\sigma}_8^{N1} = \frac{1}{z_f^3Q[Q^2(-1+\hat{x})+m_{J/\psi}^2\hat{x}]^2[m_{J/\psi}^2\hat{x}+Q^2(1+\hat{x}-z_f)]^2}$$
$$\times 128 m_{J/\psi}^2\hat{x}^2\Big(-Q^6(-1+\hat{x})z_f^2+2m_{J/\psi}^6\hat{x}^3(1-3z_f+2z_f^2)$$
$$+m_{J/\psi}^4Q^2\hat{x}^2(1-3z_f+2z_f^2)[-3z_f+2\hat{x}(1+z_f)]+m_{J/\psi}^2Q^4\hat{x}z_f[z_f(-1-2z_f+2z_f^2)$$
$$+\hat{x}^2(2-6z_f+4z_f^2)+\hat{x}(-1+z_f+4z_f^2-4z_f^3)]\Big) \qquad \text{(A.10)}$$

$$\hat{\sigma}_9^{N1} = \frac{128 m_{J/\psi}^4 P_T \hat{x}^3}{z_f^2 Q^2 [Q^2(-1+\hat{x}) + m_{J/\psi}^2 \hat{x}]^2 [m_{J/\psi}^2 \hat{x} + Q^2(1+\hat{x}-z_f)]^2}$$
$$\Big(2m_{J/\psi}^4 \hat{x}^2(-1+z_f) + 2m_{J/\psi}^2 Q^2 \hat{x}(-1+z_f)(\hat{x}-z_f+2\hat{x}z_f) + Q^4 z_f[4\hat{x}^2(-1$$
$$+z_f) + z_f - 4\hat{x}(-1+z_f)z_f]\Big) \tag{A.11}$$

(3) Hard cross sections of $N(x,0)$ in (3.44)

$$\hat{\sigma}_1^{N2} = \frac{1}{(1-z_f) z_f^2 Q^2 [Q^2(-1+\hat{x}) + m_{J/\psi}^2 \hat{x}]^3 [m_{J/\psi}^2 \hat{x} + Q^2(1+\hat{x}-z_f)]^3}$$
$$\times 128 m_{J/\psi}^2 P_T \hat{x}^3 \Big(2m_{J/\psi}^{10} \hat{x}^4 (9 - 10z_f + 7z_f^2) + 4Q^{10}(-1+\hat{x}) z_f [3 - 13z_f$$
$$+13z_f^2 - 5z_f^3 + \hat{x}^3(-3+6z_f) + \hat{x}^2(-2+9z_f-12z_f^2) + \hat{x}z_f(3-5z_f+6z_f^2)]$$
$$+2m_{J/\psi}^8 Q^2 \hat{x}^3 [-2z_f(13-14z_f+9z_f^2) + \hat{x}(-21+118z_f-117z_f^2+50z_f^3)]$$
$$+m_{J/\psi}^6 Q^4 \hat{x}^2 [42 - 90z_f + 131z_f^2 - 89z_f^3 + 42z_f^4 - 4\hat{x}z_f(-27+143z_f-142z_f^2$$
$$+58z_f^3) + 6\hat{x}^2(-23+72z_f-31z_f^2-14z_f^3+16z_f^4)] + m_{J/\psi}^4 Q^6 \hat{x}[z_f(-94+206z_f$$
$$-209z_f^2+105z_f^3-32z_f^4) - 4\hat{x}^2 z_f(-46+133z_f-11z_f^2-76z_f^3+48z_f^4) + 2\hat{x}^3($$
$$-39+32z_f+205z_f^2-234z_f^3+96z_f^4) + 2\hat{x}(-17+145z_f-345z_f^2+514z_f^3$$
$$-361z_f^4+118z_f^5)] + m_{J/\psi}^2 Q^8[-4+12z_f+37z_f^2-106z_f^3+109z_f^4-52z_f^5$$
$$+12z_f^6 + 4\hat{x}^4 z_f(-31+93z_f-71z_f^2+24z_f^3) - 4\hat{x}^3 z_f(-7-27z_f+152z_f^2-134z_f^3$$
$$+48z_f^4) + \hat{x}z_f(96-572z_f+1041z_f^2-969z_f^3+460z_f^4-104z_f^5)$$
$$+\hat{x}^2(20-92z_f+211z_f^2-199z_f^3+316z_f^4-244z_f^5+96z_f^6)]\Big) \tag{A.12}$$

$$
\begin{aligned}
\hat{\sigma}_2^{N2} \;=\; & \frac{1}{(1-z_f)z_f^2[Q^2(-1+\hat{x})+m_{J/\psi}^2\hat{x}]^3[m_{J/\psi}^2\hat{x}+Q^2(1+\hat{x}-z_f)]^3} \\
& \times 512 m_{J/\psi}^2 P_T \hat{x}^3\Big(Q^8(-1+\hat{x})^2 z_f^2(5+3\hat{x}^2+\hat{x}(4-6z_f)-6z_f+3z_f^2)+m_{J/\psi}^8\hat{x}^4(\\
& -8+40z_f-45z_f^2+16z_f^3)+2m_{J/\psi}^6Q^2\hat{x}^3[z_f(9-46z_f+51z_f^2-18z_f^3)+\hat{x}(-8 \\
& +36z_f-22z_f^2-8z_f^3+8z_f^4)]+m_{J/\psi}^4Q^4\hat{x}^2[-8+48z_f-106z_f^2+160z_f^3 \\
& -121z_f^4+36z_f^5+2\hat{x}z_f(10-45z_f+11z_f^2+28z_f^3-16z_f^4)+\hat{x}^2(-8+24z_f \\
& +50z_f^2-80z_f^3+32z_f^4)]+2m_{J/\psi}^2Q^6\hat{x}z_f[7-45z_f+84z_f^2-79z_f^3+38z_f^4-8z_f^5 \\
& +\hat{x}^3(-4+26z_f-24z_f^2+8z_f^3)+\hat{x}^2(1-43z_f^2 \\
& +46z_f^3-16z_f^4)+\hat{x}(-4+19z_f-17z_f^2+25z_f^3-22z_f^4+8z_f^5)]\Big)
\end{aligned}
\tag{A.13}
$$

$$
\begin{aligned}
\hat{\sigma}_3^{N2} \;=\; & \frac{-1}{z_f^3Q(Q^2(-1+\hat{x})+m_{J/\psi}^2\hat{x})^3(m_{J/\psi}^2\hat{x}+Q^2(1+\hat{x}-z_f))^3} \\
& \times 128 m_{J/\psi}^2\hat{x}^2\Big(2m_{J/\psi}^{10}\hat{x}^5(25-37z_f+18z_f^2)+Q^{10}(-1+\hat{x})^2z_f^2[-9+12\hat{x}^3 \\
& +\hat{x}^2(10-24z_f)+15z_f-6z_f^2+\hat{x}(5-12z_f+12z_f^2)]+m_{J/\psi}^8Q^2\hat{x}^4[z_f(-149 \\
& +217z_f-106z_f^2)+2\hat{x}(43+16z_f-79z_f^2+50z_f^3)]+m_{J/\psi}^6Q^4\hat{x}^3[54-160z_f \\
& +346z_f^2-339z_f^3+144z_f^4-\hat{x}z_f(163+187z_f-454z_f^2+256z_f^3) \\
& +\hat{x}^2(22+284z_f-294z_f^2+44z_f^3+64z_f^4)]+m_{J/\psi}^2Q^8\hat{x}z_f[12+75z_f-268z_f^2 \\
& +312z_f^3-166z_f^4+40z_f^5+2\hat{x}^4(-1+77z_f-78z_f^2+32z_f^3)+\hat{x}^3(7-137z_f \\
& -150z_f^2+256z_f^3-128z_f^4)+\hat{x}(1-184z_f+487z_f^2-602z_f^3+354z_f^4-104z_f^5) \\
& +\hat{x}^2(-18+92z_f+87z_f^2-30z_f^3-60z_f^4+64z_f^5)]+m_{J/\psi}^4Q^6\hat{x}^2[z_f(-153+443z_f \\
& -562z_f^2+362z_f^3-114z_f^4)+2\hat{x}^3(-7+88z_f+21z_f^2-106z_f^3+64z_f^4)-\hat{x}^2z_f(7 \\
& +527z_f-434z_f^2+128z_f^4)+\hat{x}(-10+142z_f-263z_f^2+608z_f^3-602z_f^4+260z_f^5)]\Big)
\end{aligned}
\tag{A.14}
$$

$$\hat{\sigma}_4^{N2} = \frac{-1}{z_f^2 Q^2[Q^2(-1+\hat{x})+m_{J/\psi}^2\hat{x}]^3[m_{J/\psi}^2\hat{x}+Q^2(1+\hat{x}-z_f)]^3}$$
$$\times 128 m_{J/\psi}^4 P_T \hat{x}^3\Big(6m_{J/\psi}^8\hat{x}^4(-3+z_f)+2m_{J/\psi}^6Q^2\hat{x}^3[2(11-3z_f)z_f+\hat{x}(-11$$
$$-31z_f+18z_f^2)]+m_{J/\psi}^4Q^4\hat{x}^2[-22+40z_f-67z_f^2+18z_f^3+8\hat{x}z_f(2+21z_f$$
$$-11z_f^2)+2\hat{x}^2(5-63z_f+6z_f^2+16z_f^3)]+Q^8z_f[4\hat{x}^4(4-15z_f+8z_f^2)+3z_f(-11$$
$$+23z_f-16z_f^2+4z_f^3)-8\hat{x}^3(1-13z_f^2+8z_f^3)+\hat{x}(-8+88z_f-153z_f^2+124z_f^3$$
$$-40z_f^4)+\hat{x}^2(16-43z_f-36z_f^3+32z_f^4)]+m_{J/\psi}^2Q^6\hat{x}[z_f(58-112z_f$$
$$+89z_f^2-24z_f^3)-4\hat{x}^2z_f(9-45z_f-4z_f^2+16z_f^3)+2\hat{x}^3(7$$
$$-21z_f-42z_f^2+32z_f^3)+2\hat{x}(5-36z_f+57z_f^2-103z_f^3+46z_f^4)]\Big) \quad \text{(A.15)}$$

$$\hat{\sigma}_8^{N2} = \frac{-1}{z_f^3 Q[Q^2(-1+\hat{x})+m_{J/\psi}^2\hat{x}]^3[m_{J/\psi}^2\hat{x}+Q^2(1+\hat{x}-z_f)]^3}$$
$$128 m_{J/\psi}^2\hat{x}^2\Big(-Q^{10}(-1+\hat{x})^2z_f^2(3+2\hat{x}^2+\hat{x}(5-4z_f)-5z_f+2z_f^2)+2m_{J/\psi}^{10}\hat{x}^5(1$$
$$-3z_f+2z_f^2)+m_{J/\psi}^6Q^4\hat{x}^3[6-24z_f+50z_f^2-53z_f^3+24z_f^4+\hat{x}z_f(-21$$
$$+27z_f+2z_f^2-16z_f^3)+6\hat{x}^2(1-2z_f-z_f^2+2z_f^3)]+m_{J/\psi}^8Q^2\hat{x}^4[z_f(-11+23z_f$$
$$-14z_f^2)+2\hat{x}(3-8z_f+3z_f^2+2z_f^3)]$$
$$+m_{J/\psi}^2Q^8\hat{x}z_f[\hat{x}^4(2-6z_f+4z_f^2)+\hat{x}^3(1-23z_f+30z_f^2-16z_f^3)$$
$$+z_f(17-56z_f+64z_f^2-34z_f^3+8z_f^4)+\hat{x}^2(6-24z_f+53z_f^2-46z_f^3+20z_f^4)$$
$$-\hat{x}(9-36z_f+31z_f^2+2z_f^3-14z_f^4+8z_f^5)]+m_{J/\psi}^4Q^6\hat{x}^2[2\hat{x}^3(1-7z_f^2$$
$$+6z_f^3)-\hat{x}^2z_f(9+17z_f-46z_f^2+32z_f^3)+z_f(-19+73z_f$$
$$-102z_f^2+70z_f^3-22z_f^4)+\hat{x}(6-18z_f+27z_f^2-4z_f^3-22z_f^4+20z_f^5)]\Big) \quad \text{(A.16)}$$

$$\begin{aligned}\hat{\sigma}_9^{N2} &= \frac{-1}{z_f^2 Q^2[Q^2(-1+\hat{x})+m_{J/\psi}^2\hat{x}]^3[m_{J/\psi}^2\hat{x}+Q^2(1+\hat{x}-z_f)]^3} \\ &\times 128 m_{J/\psi}^4 P_T \hat{x}^3\Big(2m_{J/\psi}^8\hat{x}^4(-1+z_f)+2m_{J/\psi}^6 Q^2\hat{x}^3[-2(-2+z_f)z_f+\hat{x}(-3 \\ &+z_f+2z_f^2)]+m_{J/\psi}^4 Q^4\hat{x}^2[-6+12z_f-17z_f^2+6z_f^3+6\hat{x}^2(-1-z_f+2z_f^2) \\ &-4\hat{x}z_f(-3-4z_f+4z_f^2)]+Q^8 z_f[4\hat{x}^4(-1+z_f)-4\hat{x}^3(1-6z_f+4z_f^2)+z_f(-11 \\ &+23z_f-16z_f^2+4z_f^3)+\hat{x}^2(-12+31z_f-44z_f^2+20z_f^3)+\hat{x}(4- \\ &15z_f^2+20z_f^3-8z_f^4)]+m_{J/\psi}^2 Q^6\hat{x}[4\hat{x}^2(11-8z_f)z_f^2+2\hat{x}^3(-1-5z_f+6z_f^2)+z_f(14 \\ &-32z_f+27z_f^2-8z_f^3)+2\hat{x}(-3+7z_f^2-19z_f^3+10z_f^4)]\Big) \qquad \text{(A.17)}\end{aligned}$$

(4) Hard cross sections of $N(x, Ax)$ in (3.44)

$$\begin{aligned}\sigma_1^{N3} &= \frac{-1}{(1-z_f)z_f^2[Q^2(-1+\hat{x})+\hat{x}m_{J/\psi}^2]^3[Q^2(1+\hat{x}-z_f)+\hat{x}m_{J/\psi}^2]^3} \\ &\times 128 Q^2 P_T \hat{x}^3 m_{J/\psi}^2\Big(4Q^6(-1+\hat{x})(-2+z_f)z_f[-z_f+\hat{x}(-1+2z_f)] \\ &+m_{J/\psi}^2 Q^4[-8+25z_f-50z_f^2+53z_f^3-32z_f^4+8z_f^5+\hat{x}^2(-4+103z_f \\ &-365z_f^2+446z_f^3-240z_f^4+48z_f^5)-\hat{x}(4+48z_f-275z_f^2+383z_f^3-224z_f^4+48z_f^5)] \\ &+Q^2 m_{J/\psi}^4\hat{x}[-2+50z_f-83z_f^2+59z_f^3-16z_f^4+\hat{x}(70-300z_f+396z_f^2 \\ &-226z_f^3+48z_f^4)]+m_{J/\psi}^6\hat{x}^2(-22+37z_f-27z_f^2+8z_f^3)\Big) \qquad \text{(A.18)}\end{aligned}$$

$$\begin{aligned}\sigma_2^{N3} &= \frac{-1}{(1-z_f)z_f^2[Q^2(-1+\hat{x})+\hat{x}m_{J/\psi}^2]^3[Q^2(1+\hat{x}-z_f)+\hat{x}m_{J/\psi}^2]^3} \\ &512 Q^4 P_T \hat{x}^3(-2+z_f)m_{J/\psi}^2\Big(Q^4(-1+\hat{x})^2 z_f^2+2m_{J/\psi}^2 Q^2(-1+\hat{x})\hat{x}z_f(-2+11z_f \\ &-12z_f^2+4z_f^3)+m_{J/\psi}^4\hat{x}^2(-4+20z_f-23z_f^2+8z_f^3)\Big) \qquad \text{(A.19)}\end{aligned}$$

$$\sigma_3^{N3} = \frac{1}{z_f^3[Q^2(-1+\hat{x})+\hat{x}m_{J/\psi}^2]^3[Q^2(1+\hat{x}-z_f)+\hat{x}m_{J/\psi}^2]^3}$$
$$\times 256Q^3\hat{x}^3m_{J/\psi}^2\Big(2Q^6(-1+\hat{x})^2(-2+z_f)z_f^2+m_{J/\psi}^2Q^4z_f[-1-18z_f+41z_f^2$$
$$-32z_f^3+8z_f^4-2\hat{x}(1-41z_f+76z_f^2-52z_f^3+12z_f^4)+\hat{x}^2(3-64z_f+111z_f^2$$
$$-72z_f^3+16z_f^4)]+m_{J/\psi}^4Q^2\hat{x}[1+43z_f-91z_f^2+67z_f^3-16z_f^4+\hat{x}(7-91z_f$$
$$+161z_f^2-107z_f^3+24z_f^4)]+m_{J/\psi}^6\hat{x}^2(-25+50z_f-35z_f^2+8z_f^3)\Big) \quad \text{(A.20)}$$

$$\sigma_4^{N3} = \frac{1}{z_f^2[Q^2(-1+\hat{x})+\hat{x}m_{J/\psi}^2]^3[Q^2(1+\hat{x}-z_f)+\hat{x}m_{J/\psi}^2]^3}$$
$$\times 128Q^2P_T\hat{x}^3m_{J/\psi}^4\Big(Q^4z_f[3-3z_f+\hat{x}(12-67z_f+64z_f^2-16z_f^3)+\hat{x}^2(-15$$
$$+70z_f-64z_f^2+16z_f^3)]+m_{J/\psi}^2Q^2\hat{x}[-2-16z_f+11z_f^2+2\hat{x}(-7+43z_f$$
$$-37z_f^2+8z_f^3)]+m_{J/\psi}^4\hat{x}^2(18-11z_f)\Big) \quad \text{(A.21)}$$

$$\sigma_8^{N3} = -\frac{256Q^3\hat{x}^3(1-z_f)^2m_{J/\psi}^4[Q^2(-1+\hat{x})z_f+\hat{x}m_{J/\psi}^2]}{z_f^3[Q^2(-1+\hat{x})+\hat{x}m_{J/\psi}^2]^2[Q^2(1+\hat{x}-z_f)+\hat{x}m_{J/\psi}^2]^3} \quad \text{(A.22)}$$

$$\sigma_9^{N3} = -\frac{128Q^2P_T\hat{x}^3m_{J/\psi}^4\Big(Q^2z_f[1-z_f+\hat{x}(-3+2z_f)]+m_{J/\psi}^2\hat{x}(-2+z_f)\Big)}{z_f^2[Q^2(-1+\hat{x})+\hat{x}m_{J/\psi}^2]^2[Q^2(1+\hat{x}-z_f)+\hat{x}m_{J/\psi}^2]^3} \quad \text{(A.23)}$$

(5) Hard cross sections of $N(x,(1-A)x)$ in (3.44)

$$\sigma_1^{N4} = \frac{1}{(1-z_f)z_f^2[Q^2(-1+\hat{x})+\hat{x}m_{J/\psi}^2]^3[Q^2(1+\hat{x}-z_f)+\hat{x}m_{J/\psi}^2]^3}$$
$$\times 128Q^2P_T\hat{x}^3m_{J/\psi}^2\Big(4Q^6(-1+\hat{x})z_f[-1+6z_f-3z_f^2+\hat{x}(3-9z_f+4z_f^2)]+$$
$$m_{J/\psi}^2Q^4[-8+15z_f-34z_f^2+37z_f^3-24z_f^4+6z_f^5+\hat{x}(4-80z_f+361z_f^2$$
$$-449z_f^3+248z_f^4-52z_f^5)+\hat{x}^2(-4+101z_f-379z_f^2+446z_f^3-236z_f^4+48z_f^5)]$$
$$+m_{J/\psi}^4Q^2\hat{x}[2+46z_f-69z_f^2+49z_f^3-12z_f^4+\hat{x}(70-310z_f+400z_f^2$$
$$-236z_f^3+52z_f^4)]+m_{J/\psi}^6\hat{x}^2(-22+33z_f-25z_f^2+6z_f^3)\Big) \quad \text{(A.24)}$$

$$\sigma_2^{N4} = \frac{1}{(1-z_f)z_f^2[Q^2(-1+\hat{x})+\hat{x}m_{J/\psi}^2]^3[Q^2(1+\hat{x}-z_f)+\hat{x}m_{J/\psi}^2]^3}$$
$$\times 1024Q^4P_T\hat{x}^3(-2+z_f)m_{J/\psi}^2\Big(Q^4(-1+\hat{x})^2z_f^2+2m_{J/\psi}^2Q^2(-1+\hat{x})\hat{x}z_f(-1$$
$$+6z_f-6z_f^2+2z_f^3)+m_{J/\psi}^4\hat{x}^2(-2+10z_f-11z_f^2+4z_f^3)\Big) \quad \text{(A.25)}$$

$$\sigma_3^{N4} = \frac{-1}{z_f^3[Q^2(-1+\hat{x})+\hat{x}m_{J/\psi}^2]^3[Q^2(1+\hat{x}-z_f)+\hat{x}m_{J/\psi}^2]^3}$$
$$\times 128Q^3\hat{x}^2m_{J/\psi}^2\Big(Q^6(-1+\hat{x})^2z_f^2[3-3z_f+\hat{x}(-13+8z_f)]+m_{J/\psi}^2Q^4\hat{x}z_f[-2$$
$$-55z_f+112z_f^2-80z_f^3+20z_f^4-4\hat{x}z_f(-46+83z_f-55z_f^2+13z_f^3)+\hat{x}^2(2-129z_f$$
$$+220z_f^2-140z_f^3+32z_f^4)]+m_{J/\psi}^4Q^2\hat{x}^2[-2+110z_f-215z_f^2+157z_f^3-40z_f^4$$
$$+\hat{x}(14-184z_f+319z_f^2-216z_f^3+52z_f^4)]+m_{J/\psi}^6\hat{x}^3(-50+102z_f-77z_f^2+20z_f^3)\Big)$$
$$\text{(A.26)}$$

$$\begin{aligned}\sigma_4^{N4} &= \frac{-1}{z_f^2(Q^2(-1+\hat{x})+\hat{x}m_{J/\psi}^2)^3(Q^2(1+\hat{x}-z_f)+\hat{x}m_{J/\psi}^2)^3}\\ &\times 128Q^2P_T\hat{x}^3m_{J/\psi}^4\Big(Q^4z_f[\hat{x}(12-65z_f+68z_f^2-20z_f^3)\\ &+3(-1+5z_f-6z_f^2+2z_f^3)+\hat{x}^2(-17+66z_f-60z_f^2+16z_f^3)]\\ &+m_{J/\psi}^2Q^2\hat{x}[2-32z_f+37z_f^2-12z_f^3+2\hat{x}(-7+38z_f-36z_f^2+10z_f^3)]\\ &+m_{J/\psi}^4\hat{x}^2(18-19z_f+6z_f^2)\Big)\end{aligned} \tag{A.27}$$

$$\begin{aligned}\sigma_8^{N4} &= \frac{-1}{z_f^3(Q^2(-1+\hat{x})+\hat{x}m_{J/\psi}^2)^3(Q^2(1+\hat{x}-z_f)+\hat{x}m_{J/\psi}^2)^2}\\ &\times 128Q^3\hat{x}^2m_{J/\psi}^2\Big(Q^4(-1+\hat{x})^2z_f^2+2m_{J/\psi}^2Q^2(-1+\hat{x})\hat{x}z_f(-1+6z_f-6z_f^2+2z_f^3)\\ &+m_{J/\psi}^4\hat{x}^2(-2+10z_f-11z_f^2+4z_f^3)\Big)\end{aligned} \tag{A.28}$$

$$\begin{aligned}\sigma_9^{N4} &= -\frac{1}{z_f^2[Q^2(-1+\hat{x})+\hat{x}m_{J/\psi}^2]^3[Q^2(1+\hat{x}-z_f)+\hat{x}m_{J/\psi}^2]^2}128Q^2P_T\hat{x}^3m_{J/\psi}^4\\ &\Big(Q^2z_f[-1+4z_f-2z_f^2+\hat{x}(5-10z_f+4z_f^2)]+m_{J/\psi}^2\hat{x}(2-5z_f+2z_f^2)\Big)\end{aligned} \tag{A.29}$$

(6) Hard cross sections of $N(Ax, -(1-A)x)$ in (3.44)

$$\begin{aligned}\sigma_1^{N5} &= \frac{1}{(1-z_f)z_f^2[Q^2(-1+\hat{x})+\hat{x}m_{J/\psi}^2]^3[Q^2(1+\hat{x}-z_f)+\hat{x}m_{J/\psi}^2]^3}\\ &\times 256Q^2P_T\hat{x}^3m_{J/\psi}^2\Big(2Q^6(-1+\hat{x})^2z_f(1-4z_f+2z_f^2)+m_{J/\psi}^2Q^4(z_f^2(-10\\ &+17z_f-12z_f^2+3z_f^3)-2\hat{x}z_f(16-79z_f+108z_f^2-62z_f^3+13z_f^4)+2\hat{x}^2(-2+23z_f\\ &-84z_f^2+107z_f^3-59z_f^4+12z_f^5))+m_{J/\psi}^4Q^2\hat{x}(2z_f(12-20z_f+13z_f^2-3z_f^3)\\ &+\hat{x}(30-149z_f+210z_f^2-123z_f^3+26z_f^4))+m_{J/\psi}^6\hat{x}^2(-14+23z_f-14z_f^2+3z_f^3)\Big)\end{aligned} \tag{A.30}$$

$$\sigma_2^{N5} = \frac{1}{(1-z_f)z_f^2[Q^2(-1+\hat{x})+\hat{x}m_{J/\psi}^2]^3[Q^2(1+\hat{x}-z_f)+\hat{x}m_{J/\psi}^2]^3} \times 512Q^4P_T\hat{x}^3(-2+z_f)m_{J/\psi}^2\Big(Q^4(-1+\hat{x})^2z_f^2+2m_{J/\psi}^2Q^2(-1+\hat{x})\hat{x}z_f(-2+11z_f-12z_f^2+4z_f^3)+m_{J/\psi}^4\hat{x}^2(-4+20z_f-23z_f^2+8z_f^3)\Big) \quad (A.31)$$

$$\sigma_3^{N5} = \frac{-1}{z_f^3[Q^2(-1+\hat{x})+\hat{x}m_{J/\psi}^2]^3[Q^2(1+\hat{x}-z_f)+\hat{x}m_{J/\psi}^2]^3} \times 128Q^3\hat{x}^2m_{J/\psi}^2\Big(Q^6(-1+\hat{x})^2z_f^2[3-3z_f+\hat{x}(-5+4z_f)]+m_{J/\psi}^2Q^4\hat{x}z_f[-4-43z_f+106z_f^2-80z_f^3+20z_f^4-4\hat{x}(1-39z_f+79z_f^2-55z_f^3+13z_f^4)+\hat{x}^2(8-113z_f+210z_f^2-140z_f^3+32z_f^4)]+m_{J/\psi}^4Q^2\hat{x}^2[z_f(100-221z_f+163z_f^2-40z_f^3)+\hat{x}(12-166z_f+321z_f^2-222z_f^3+52z_f^4)]+m_{J/\psi}^6\hat{x}^3(-52+114z_f-83z_f^2+20z_f^3)\Big) \quad (A.32)$$

$$\sigma_4^{N5} = \frac{-1}{z_f^2(Q^2(-1+\hat{x})+\hat{x}m_{J/\psi}^2)^3(Q^2(1+\hat{x}-z_f)+\hat{x}m_{J/\psi}^2)^3} \times 256Q^2P_T\hat{x}^3(-2+z_f)m_{J/\psi}^4\Big(Q^4z_f[3(-1+z_f)z_f+2\hat{x}^2(2-7z_f+4z_f^2)-2\hat{x}(1-7z_f+5z_f^2)]+m_{J/\psi}^2Q^2\hat{x}[2(4-3z_f)z_f+\hat{x}(3-17z_f+10z_f^2)]+m_{J/\psi}^4\hat{x}^2(-5+3z_f)\Big) \quad (A.33)$$

$$\sigma_8^{N5} = \frac{-1}{z_f^3(Q^2(-1+\hat{x})+\hat{x}m_{J/\psi}^2)^3(Q^2(1+\hat{x}-z_f)+\hat{x}m_{J/\psi}^2)^3} \times 128Q^3\hat{x}^2m_{J/\psi}^2\Big(Q^6(-1+\hat{x})^2(1+\hat{x}-z_f)z_f^2+m_{J/\psi}^2Q^4\hat{x}z_f[z_f(-9+22z_f-16z_f^2+4z_f^3)+\hat{x}^2(-4+17z_f-14z_f^2+4z_f^3)-4\hat{x}(-1+2z_f+2z_f^2-3z_f^3+z_f^4)]+m_{J/\psi}^4Q^2\hat{x}^2[z_f(12-35z_f+29z_f^2-8z_f^3)+\hat{x}(-4+10z_f+3z_f^2-10z_f^3+4z_f^4)]+m_{J/\psi}^6\hat{x}^3(-4+14z_f-13z_f^2+4z_f^3)\Big) \quad (A.34)$$

$$\begin{aligned}\sigma_9^{N5} &= \frac{1}{z_f^2[Q^2(-1+\hat{x})+\hat{x}m_{J/\psi}^2]^3[Q^2(1+\hat{x}-z_f)+\hat{x}m_{J/\psi}^2]^3} \\ &\quad 256Q^2P_T\hat{x}^3(-2+z_f)(1-z_f)m_{J/\psi}^4\Big(Q^4z_f(2\hat{x}^2+z_f-2\hat{x}z_f) \\ &\quad +m_{J/\psi}^2Q^2\hat{x}(\hat{x}-2z_f+2\hat{x}z_f)+m_{J/\psi}^4\hat{x}^2\Big)\end{aligned} \tag{A.35}$$

Acknowledgment

Perhaps every graduate student has their own story when they have a first glance at research.

First and foremost, I owe my deepest gratitude to my advisor, Prof. Shinsuke Yoshida. Throughout the whole three years, he was fully supportive and helped me in all possible ways he could. Specifically, it was quite challenging for me to write this thesis in English. I could hardly ever finish it without the guidance and the support from him. Besides, I'd like to express my appreciate to Pro. Hongxi Xing for providing me assistance and companionship in the course of preparing the paper. In addition, I'll express my appreciate to teachers who have taught me at this school in the past three years. They provided me with the priceless knowledge about high energy physics and guided me to dive deep into the research.

Finally, I am really grateful to all those who devote much time to reading this thesis and give me much advice, which will benefit me in my later study.

华南师范大学学位论文原创性声明

本人郑重声明：所呈交的学位论文，是本人在导师的指导下，独立进行研究工作所取得的成果。除文中已经注明引用的内容外，本论文不包含任何其他个人或集体已经发表或撰写过的研究成果。对本文的研究做出重要贡献的个人和集体，均已在文中以明确的方式标明。

本人完全意识到本声明的法律结果由本人承担。

论文作者签名：陈隆杰

日期：2024 年 5 月 7 日

学位论文使用授权声明

本论文属于非涉密论文，本人完全了解华南师范大学有关收集、保留、使用学位论文的规定，即研究生在校攻读学位期间论文的知识产权单位属华南师范大学。学校有权保留学位论文并向国家主管部门或其指定机构送交论文的电子版和纸质版，有权将学位论文用于非赢利目的复制并允许论文进入学校图书馆、院系资料室被查阅和借阅，有权将学位论文的内容编入有关数据库进行检索，可以采用复印、缩印或其他方法保存学位论文。

论文作者签名：陈隆杰　　导师签名：Shinsuke Toshida

日期：2024 年 5 月 7 日　　日期：2024 年 5 月 6 日